AZOTERA

Non-Proprietary Technical Summary

Azotera has developed a breakthrough system to profitably produce zero-carbon ammonia at wholesale prices without subsidies. The reversible system is compact, flexible, and highly efficient — delivering backup power with storage measured in weeks, not days. This document provides the technical background that validates Azotera's performance criteria. The two core innovations are a proprietary ceramic manufacturing process for multi-material ceramic monoliths with internal gas routing and a patented high-pressure electrode patent. Combined these innovations facilitate manufacturing miniature molecule factories; a house brick sized ceramic assembly that integrates steam production, water splitting and ammonia synthesis to transform water, air and energy feedstocks into ammonia at unprecedented efficiency.

The system has multiple viable use cases including direct on-farm production of fertilizer, unsubsidized alternative fuel production for heavy transport, and data center backup power. The initial market opportunity with the highest value proposition solves two problems simultaneously: 1) critical grid stabilization with long-duration energy storage at substations, 2) reliable local production of low-cost sustainable fertilizer.

Azotera's distributed scale reversible architecture differentiates itself from other ammonia systems by operating as a utility asset rather than a utility customer. As a utility asset the system can profitably produce unsubsidized green ammonia below wholesale price of fossil derived ammonia. The 2.5MW system with 200 tons of storage is the ideal solution for ultra-long duration storage at substations. Each system delivers a $30M value stack over the 20-yr operating life:

1. 7+ days continuous backup energy reliability, displacing a 12-hr $20M battery
2. Seasonal energy arbitrage worth $6M+,
3. Ammonia offtake profits worth $15M+,
4. Carbon credits for displacing fossil ammonia worth $6M+
5. Compliance credits for offsetting fossil generation worth $3M+

This document outlines the technical innovation underpinning Azotera's technology which includes a patented vanadia doped stabilized zirconia electrode and a proprietary dry powder manufacturing method. A limited selection of performance measurements are presented. This document briefly discusses the ceramic printing Azotera is scaling from prototype to production.

These performance measurements were used in a detailed system model to extrapolate benchtop performance into an integrated system that accounts for all of the relevant physics when estimating the system performance. Critically the system performance is shown to achieve 68% energy conversion after accounting for AC/DC rectification losses, nitrogen generation and compression parasitic loss, inert gas purge and refrigeration loads associated with condensing out the ammonia product.

The cost estimation section outlines the projected cost for the materials production, brick manufacturing, and balance of plant systems. This leads into the market analysis section which highlights the value proposition in the ag market, utility market and renewable energy firming markets that would allow 80% gross margin sales. The final section walks through the technical risks in scaling this technology from the existing demonstrations to a full-scale prototype.

Contents

Company Description

Azotera developed a breakthrough ceramic manufacturing process for multi-material ceramic monoliths with internal gas routing. Combined with a high-pressure electrode patent, this process manufactures miniature molecule factories; a house brick sized ceramic assembly that integrates steam production, water splitting and ammonia synthesis to transform water, air and energy feedstocks into ammonia at unprecedented efficiency. The company will bring to market a revolutionary distributed scale ammonia plant for low-cost production of anhydrous ammonia fertilizer and grid stabilizing power. The system will create a cost-effective pathway for unsubsidized use of zero-carbon ammonia as a heavy transport fuel, and data center backup power.

Leadership Team

Dr. Dustin McLarty
Chief Technical Officer

- 18 years of Solid-Oxide R&D
- 25+ papers, 1000+ citations
- PI on over $4million
- Tenured Associate Professor
- Fulbright Scholar
- Professional Triathlete
- USA Swimming National Team

Christopher E. Wood
Chief Executive Officer

- 30+ years as operator, investor
- Rapid workforce expansion
- Facilities build-out
- Digital fabrication methods
- Expert in the implementation of Lean production systems
- Partner of one of the largest WA wheat farms

Dustin McLarty – Founder & Chief Technical Officer

When pursuing his PhD, Dr. McLarty was inspired to transition from rocket engine development to electrochemical energy conversion. Trained in systems integration and controls, specifically for high temperature pressurized fuel cells and electrolysis systems, Dr. McLarty served as a Fulbright fellow before accepting a faculty position at Washington State University (WSU). At WSU he served as PI on grants for the DOE, ARPA-E and DARPA totaling $3.8M and collaborated on DOE and NSF grants totaling an additional $6.2M. He also conducted industrial research for different fuel cell technology companies totaling $1.2M.

Within the ARPA-E INTEGRATE program, Dr. Mclarty invented the vanadia co-doped electrode material and developed the VYZion monolith concept to address the constraints in manufacturing

and solid oxide system operation, performance, and cost identified from years of research. He left his tenured faculty position at the end of 2024 to focus all efforts on commercializing this technology. He has bootstrapped Azotera through the initial facility buildout stage with a combination of grants, contracts and test equipment sales, while demonstrating that the laboratory proof-of-concept pieces could be fabricated using industrially relevant manufacturing methods.

Christopher E. Wood – Co-Founder and Chief Executive Officer

Christopher E. Wood brings over three decades of transformative leadership in advanced manufacturing, energy systems, and technology commercialization to Azotera. As the former Vice President of Operations for Skywalker Holdings' NorCal Museum Siding division, he led one of the most complex composite manufacturing startups in the country—delivering more than 1,200 unique engineered façade panels for the Lucas Museum of Narrative Art in just 36 months. This achievement required rapid workforce expansion, facilities build-out, implementation of advanced digital fabrication methods, adoption of Lean/TPS principles, and coordination across aerospace, automotive, construction, and advanced-materials industry standards.

A seasoned operator, investor, and startup strategist, Wood has scaled multiple new-technology ventures through early-stage development, capital formation, and product launch. His background spans clean-tech manufacturing, automotive, aerospace, high-precision industrial equipment, large-scale fabrication technologies, oilfield machinery, and agricultural and timber operations—giving him a rare ability to combine engineering rigor with commercial execution.

At Azotera, he provides senior-level guidance across R&D scaling, manufacturing design, supply-chain strategy, capital-stack structuring, and stakeholder engagement. His track record of turning novel technologies into bankable, deployable products positions him as a critical strategic force in moving Azotera from laboratory innovation to revenue-generating deployment.

Technical Advisors

Bill Fuglevand

Former CarbonQuest CTO, Avista Labs founder with 20+ patents specializing in hydrogen, CO_2 capture, and renewable energy.

John Gibson

Chief R&D Engineer at Avista Utilities, leading grid initiatives including DMS automation, energy storage, microgrids, and Spokane's eco-district.

David Peterson

Former Electrolysis Team Lead and Hydrogen Production Program Manager, Hydrogen and Fuel Cell Technologies Office, Department of Energy

Jack Brouwer

Director of the Clean Energy Institute at the University of California, Irvine and Chancellor's Fellow of Engineering

Problem

Utilities face crushing demands to accommodate hyper-scale data centers and large green ammonia plants without impacting existing ratepayers. The capacity limits for electricity transmission and the non-coincidence of supply and demand cause tremendous electric price volatility and constrain additional renewable energy deployments. The only available technologies for utilities to maintain reliability are i) batteries with only a few hours of capacity, ii) distributed generators that are expensive, noisy and polluting, and iii) large peaking plants that face monumental costs and extended timelines. Electric utilities need a zero-carbon energy storage solution with days or weeks of capacity rather than hours.

The proposed 1000 tpd green ammonia production facilities rely on subsidies, regulations, and green premiums. The PEM and Alkaline electrolyzer facilities require 24/7 stable operation to avoid premature degradation, integrate with the large-scale Haber-Bosch synthesis loops, and amortize CAPEX. They must pay for firm electric power and offset energy feedstock emissions with the purchase of carbon credits to meet emission intensity standards. The hydrogen compressors consume too much energy and require too much maintenance. Make-up heating to replace the SMR reactor waste heat raises energy consumption to 10-12 MWh/ton. The production cost before considering capital investment and operating expenses exceeds blue ammonia by 50%-100%.

Solution

Azotera addresses the utility challenge with a distributed scale ammonia synthesis plant that also addresses the cost of green ammonia. Azotera's patented electrode material and DPP-AM manufacturing process produces a low-cost ceramic monolith that combines thermochemistry and electrochemistry to produce ammonia 40% more efficiently than existing electrolysis methods. The modular systems have the flexibility to transition into a generator providing backup power when the grid needs it most. The systems can profitably sell ammonia below 450 $/ton wholesale prices, reducing fertilizer costs 30% after accounting for local storage and distribution. A single ammonia trailer holds 150MWh of energy, 15x the capacity and 1/30th the cost of 10MWh batteries deployed by utilities today. Distributed scale ammonia production at existing substations avoids permitting and grid connection delays, minimizes distribution costs, and isolates farmers from global energy market price volatility. Azotera's technology supports grid resilience, decarbonizes food production, and lowers fertilizer costs for American farmers.

Figure 1. Azotera 's energy solution combining distributed ammonia production with reliable backup generation

Azotera's efficiency stems from pumping liquid water instead of compressing hydrogen which avoids 15% of the total energy consumption and more than 20% of the equipment and maintenance cost, and from directly recovering synthesis heat which avoids an additional 20% of the energy consumption. Azotra's system consumes a mere 7.5 MWh/ton, nearly 70% conversion efficiency. The design unlocks a development path that scales like Moore's Law: i) doubling the pressure doubles the active surface area via half-height channels, and ii) higher pressure increases surface activity. Doubling pressure improves output 4x in a continuously reinforcing feedback loop.

Azotera's System

Technical Background

Traditional natural gas fueled Haber-Bosch ammonia plants can be described as consisting of six major capital components. Traditional ammonia production uses 28-33 GJ natural gas and 0.6 to 1.0 MWh electricity per ton ammonia. This equates to a net 46-57% LHV efficiency, assuming on-site electric generation at 50% from natural gas.

SMR reactor and hydrogen purification: Flowing heated steam and natural gas at 10-30 bar and between 600°C and 900°C over Nickel catalyst breaks the methane down to H2, CO and CO2. High temperature, 350°C-400°C, and low temperature, 200°C-250°C, shift reactors convert the CO to CO2 and additional H2. An amine scrubber, typically monoethanolamine (MEA), binds with 95% of the CO2 to form carbamate. Re-heating to 300°C-400°C over a Nickel catalyst induces methanation to convert the remaining 5% CO2 and some CO to CH4 to avoid poisoning the catalyst.

1) **Hydrogen Compression:** Typically, 4-6 intercooled stages of reciprocating compressors boosting pressure from 20 bar to 150bar.
2) **Nitrogen production:** Cryogenic air separation at large plants results in high purity. The oxygen stream is used for the SMR heating, e.g. oxycombustion. Small plants may use pressure swing absorption (PSA)
3) **Nitrogen Compression:** Multi-stage intercooled compressors to raise nitrogen from 5-7 bar to 150-200 bar.
4) **Ammonia Synthesis Reactor:** Nitrogen and hydrogen at 150bar and a 3:1 ratio are heated to 400°C. Traditionally uses an iron-based catalyst (Fe promoted with K_2O, Al_2O_3, CaO), or Ruthenium and MgO in modern reactors at lower temperature and pressure. 15-20% of nitrogen is converted in a 3-stage packed bed reactor with intermediate quenching to control the exothermic heat of the synthesis reaction. Gases must be looped through reactor and refrigeration 5-8 times, requiring re-compression.
5) **Refrigeration and collection:** After recovering some available waste heat the synthesis gas is cooled to -25C with a refrigerant system. A tank separates the liquid ammonia from the gaseous hydrogen and nitrogen.

Table 1. Summary of ammonia production inefficiencies.

	Traditional	Green Ammonia	Azotera 's System
Hydrogen Production	25% loss	15-40%	15%
Hydrogen Compression	4% loss	12%	0%
Nitrogen Production	3-7%	3-8%	3%
Nitrogen Compression	2-3%	2-4%	2%
Ammonia Synthesis	8-11%	8-12%	8%
Refrigeration & Collection	2-4%	2-5%	2%
Summary	46-57% Efficient	30-49% Efficient	70% Efficient

Most proposed green ammonia plants retain the six large CAPEX components but replace the SMR and hydrogen purification with an electrolyzer. PEM and alkaline electrolyzers operate at 51-55 kWh per kg hydrogen while newer solid oxide systems operate between 37 and 42 kWh per kg hydrogen. All electrolyzers generally operate at lower pressure than SMR systems, substantially increasing the hydrogen compression parasitic. The net operating efficiency ranges from 42-49%.

Figure 2 illustrates the basic arrangement of a green ammonia plant. The three hot systems comprise the bulk of the cost and inefficiency. Azotera combines these hot elements into a single ceramic monolith packed with microchannels for electrolysis, synthesis and heat exchange. The resulting impact on CAPEX and efficiency is significant. The primary differences with Azotera's system are that the hydrogen production occurs at pressure near the thermoneutral voltage to maintain high efficiency and eliminate hydrogen compression losses. The nitrogen production uses PSA and similar intercooled compressors to other small ammonia plants. The integrated synthesis reactor captures additional waste heat. Refrigeration load is reduced because microchannels can increase the yield on each synthesis loop. The plant is simplified to only four major CAPEX systems because the monolith covers hydrogen production & compression and synthesis

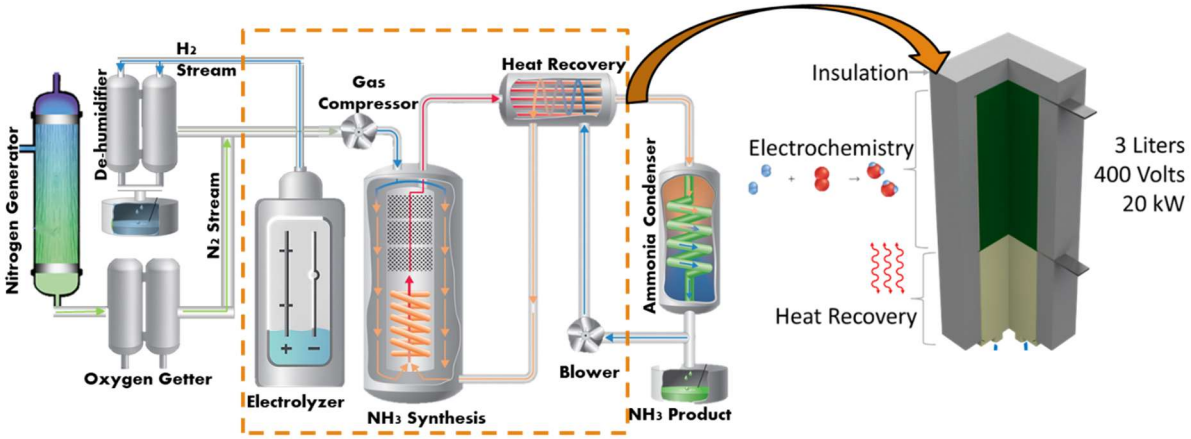

Figure 2. Azotera's innovative monolith integrates the electrolysis, synthesis and heat recovery elements.

The research literature discusses direct nitrogen reduction technologies using low-temperature low-pressure operating conditions combined with novel synthesis catalysts and ammonia sorbents to push past the equilibrium limits. These approaches lack sufficient production rates because the synthesis reaction naturally lends itself towards process intensification. Azotera's ceramic monolith technology recovers energy by directly integrating electrochemistry and thermochemistry steps. This additional process intensification will allow a small distributed system to produce ammonia more efficiently than existing large-scale systems without incurring unrealistic CAPEX challenges of these novel direct nitrogen reduction technologies.

Table 2. Summary of ammonia synthesis pathways

Technology	Net Efficiency	Cost	Challenge
SMR + Haber-Bosch	66% (7.8 MWh/ton)	400 $/ton	CO_2 emissions (grey) and fossil fuel use (blue)
PEM + Haber-Bosch	43-51% (10-12 MWh/ton)	1,200 $/ton	Requires expensive firm renewable power
Azotera 's Green Bricks	70% (7.5 MWh/ton)	<400 $/ton	Scaling production & validating performance

The unprecedented ammonia synthesis efficiency stems from three key changes in the system design and operating conditions: 1) Operation at pressure, 2) Operation without an air sweep gas, and 3) Heat recovery from ammonia synthesis.

Pressurized Electrolysis: A survey conducted of existing hydrogen fueling stations found an average isothermal compression efficiency of 45% for entire compressor systems including intercooling. Figure 3 illustrates the significance of pumping liquid water and electrolyzing high pressure steam rather than compressing a gas. The switch to a high pressure electrolyzer accounts for 14% energy savings when compressing atmospheric pressure hydrogen to the 200 bar ammonia synthesis pressure.

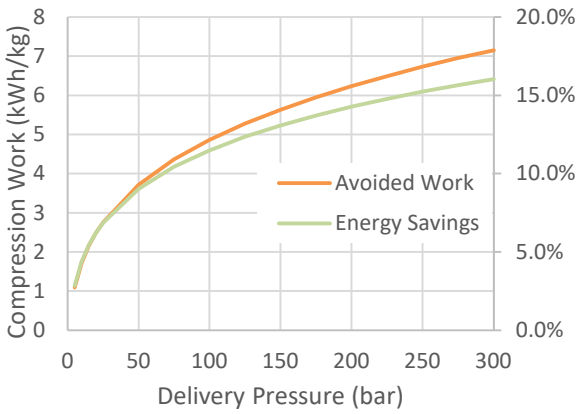

Figure 3. Avoided hydrogen compression work

Avoiding Air Sweep Gas: Pressurizing the air side of the electrolyzer would undo all of the avoided hydrogen compression work. The high-pressure steam electrolyzer must therefore operate without a sweep gas. This means the air electrode must tolerate nearly 100% oxygen at high pressure and temperature and the operating voltage must be close to the thermoneutral voltage. Figure 4 compares the reference voltage and the thermoneutral voltage at increasing pressure. A shaded band surrounding the thermoneutral voltage represents the operating window without a secondary heat transfer fluid for operation with 5% exhaust humidity. For a constant ASR, changing the pressure, humidity, or stack temperature differential constraint can narrow or expand the gap between the minimum electrolysis voltage and the operating window. This allows power modulation for responding to grid price dynamics or renewable intermittency. Without a sweep gas means the operating voltage will range from 1.20V to 1.35V. The lower operating voltage accounts for 20% of the energy savings when compared to PEM electrolysis at 1.70V.

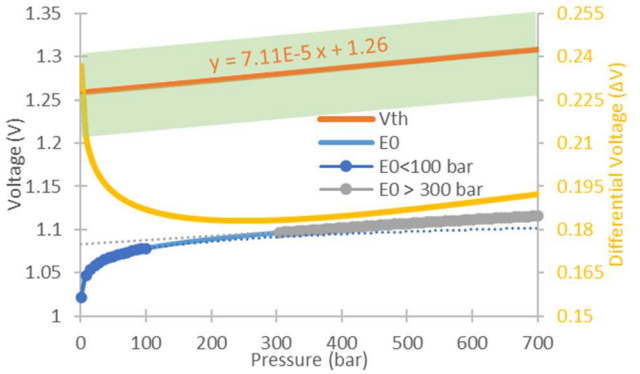

Figure 4. Pressure dependence of thermoneutral and reference voltages

Heat Recovery: The effectiveness of the heat recovery system determines the overall system energy consumption. Figure 5 presents the heat transfer requirements as a function of temperature for the water supply and composite exhaust. At all pressures the exhaust products have a lower average heat capacity. Because the partial pressure of water in the effluent stream is less than the supply, the exhaust condensing heat cannot be recovered to boil the inlet resulting in an energy recovery shortfall of 5 kWh/kg. Higher pressure reduces this shortfall. The exothermic ammonia synthesis can operate at 350°C and provide make-up heat, saving 6-8% of total energy use.

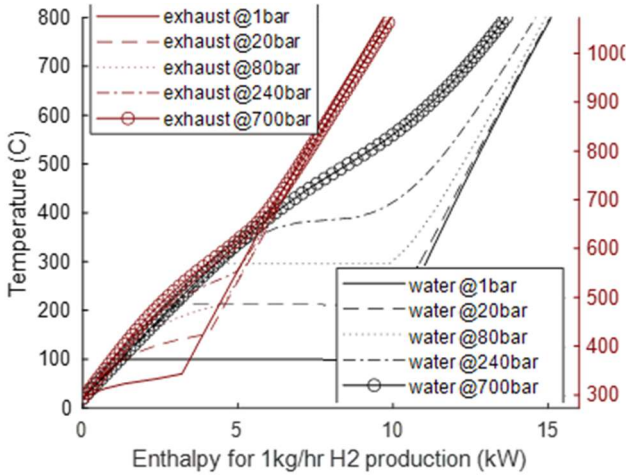

Figure 5. Thermal capacity with 33% exhaust humidity

Vanadia-Doped Stabilized Zirconia Materials

Electrolysis introduces additional challenges with the most common air side electrodes, LSM and LSCF. The high pO_2 pressures lead to formation of $SrZrO_3$ at the electrode-electrolyte interface and eventually to electrode delamination. GDC barrier layers can mitigate $SrZrO_3$ formation, but degradation remains high. Nickel fuel electrodes, commonly a Ni-YSZ cermet, tend to coke and oxidize when attempting co-electrolysis of CO_2, necessitating alternative electrodes such as LaCrO3, SrFeMoO, or LaSrTiO. Azotera patented an alternative electrode material, nano-powder vanadia-yttria stabilized zirconia (VYSZ) with distinct advantages:

- A defect-cubic structure that is chemically and structurally compatible with the 8YSZ electrolyte; preventing diffusion of electrode species into the electrolyte or interfacial voids and eliminating electrode-electrolyte activation losses caused by dissimilar conduction pathways through materials such as LSM and YSZ.
- The VYSZ material forms V_2O_3 and possibly other oxides (VO/VO_2) that provide excellent catalysis of the oxygen reaction.

The material achieves similar repeat-unit performance with common Ni-YSZ cermets and metal interconnect plates for three reasons: i) high pressure operation allows for smaller gas channels resulting in much shorter electrical conduction lengths, ii) the mixed-conducting electrode can be fully dense, increasing the cross sectional area of electrical conduction, iii) dopant-level optimization will substantially improve conductivity.

Table 3. State-of-art knowledge of vanadia doped zirconia nanoceramics

Finding	Description	Impact	Evidence
1	Exceptionally hydrophilic pre-sintering	Powder pressing requires a dry environment (~1% RH)	Mass uptake and fractures upon sintering
2	7.5% doping before secondary phase appears	Compatibility with defect cubic YSZ electrolyte.	XRD analysis, DSC
3	Higher conductivity with higher doping.	Performance improvement with increased vanadia	EIS under reducing conditions
4	Oxygen conductivity similar to 8YSZ and 12CSZ	Mixed conduction ideal for electrodes	EIS under reducing and oxidizing environments
5	Conduction in both oxidizing and reducing environments	Viable electrode in fuel and air and as interconnect	EIS under reducing and oxidizing environments
6	No short-term degradation	Exhibits stability of YSZ	Steady operation

XRD analysis shown in Figure 6 demonstrates the single cubic zirconia phase is retained with 7.5 mol.% dopant, with a secondary V_2O_3 phase appearing at higher concentrations. The secondary phase increases density, and forms a cermet with the stabilized zirconia after conditioning in air to precipitate more vanadia into the boundary space.

Synthesized nanocrystalline ceramics have shown an increased capacity for dopants accommodated in the cubic zirconia matrix due to the higher particle surface areas which act as sinks for the dopant ion. The reverse strike synthesis procedure allows sufficient vanadia in the nano-YSZ matrix to form an electrically conductive cermet. The mixed conductivity of VYSZ allows for more triple point area per gram and a larger cross section for conduction than conventionally produced porous anode cermets.

Performance Measurements

Most of Azotera's performance measurements are proprietary. This section presents some early tests that are indicative of common trends seen in the test samples. Figure 7 shows the typical break-in period. The change in current output occurs due to some conditioning of the silver paste adhered to the sample as a current collector. After the initial break-in period the sample performance is steady and 100% reversible. Figure 8 highlights the important role that pressurization plays in the operation. These tests in both electrolysis and fuel cell modes demonstrate a 4x to 8x increase in power density with benefits plateauing after 40 bar. The performance was measured with 700µm electrolyte support to withstand the large differential pressures when testing at 45 bar. Thin membranes produced by DPP-AM will improve performance 10x and while withstanding the differential pressure by spanning <0.5mm instead of the 18mm of the current pressurized button cell test apparatus. Transitioning from the compressive face seals of a single button cell to the ceramic welded connections of a monolith stack requires resources for a production scale-up to a size amenable for four gas connection points. Thus the work to date has pursued proof-of-concept demonstrations on two independent tracks i) pressurized testing on button cells and ii) manufacturing of multi-layered monoliths with internal gas routing comprised of standard and vanadia-doped YSZ.

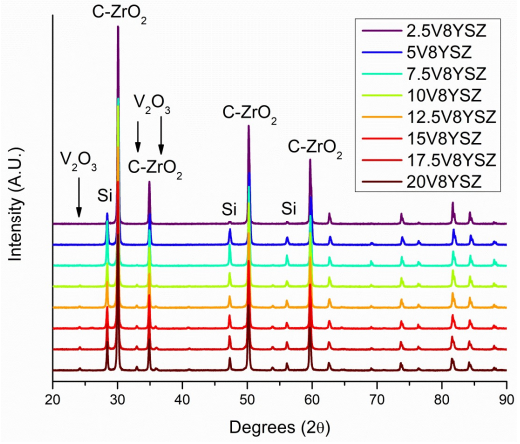

Figure 6. VYSZ x-ray diffraction data at 1200 °C in 10%H2/N2. Si standard was mixed in the powder. Only cubic ZrO2 (PDF# 30-1468) was seen below 7.5V. A small peak is seen near 10V that corresponds to V2O3 (PDF# 01-071-0347) and grows up to 20V but stays below 4 wt% at 20V

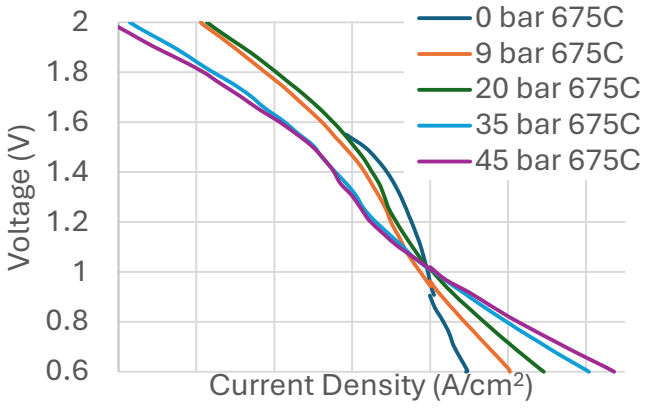

Figure 8. Cell performance trends with pressurized operation

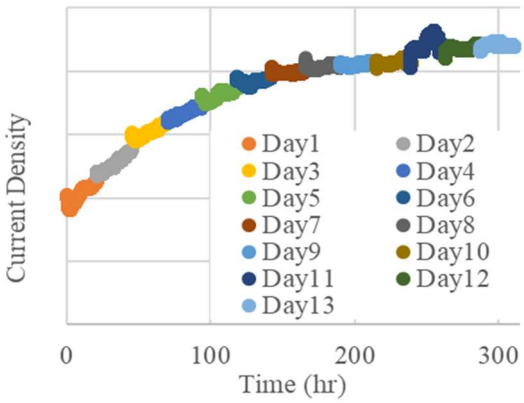

Figure 7. Durability measurements of a VYZion cell

VYZion's stable cubic zirconia structure tolerates contaminants, operates in both oxidizing and reducing environments, and remains stable at ultra-high operating pressures needed for high conversion ammonia synthesis. Validation tests have demonstrated high temperature operation up to 100 bar in both reducing and oxidizing environments for 100's of hours without degradation.

Solid Oxide Manufacturing

Solid oxide electrolysis cells (SOEC) have long held the promise for affordable and clean hydrogen production. Mass production at sufficient quantity to lower costs while retaining performance and quality control has proven elusive. The most common production technique uses tape casting, screen printing and thermal spray deposition to produce either anode or electrolyte supported cells. Stack design and assembly has proven equally challenging with two major issues being high temperature sealing between ceramic and metal materials with different coefficients of thermal expansion and low resistance electrical contact between the cell and interconnect that avoids blocking reactant gas flow. Two alternative manufacturing approaches emerged, one that fully integrates a metal cell support, and another that eliminates the metal entirely.

Metal supported cells receive the majority of the research attention due to the lower cost manufacturing and mechanical robustness. Commercial efforts to address degradation challenges primarily focus on lowering the operating temperature and retaining performance by producing ever thinner functional and barrier layers. Limited studies have deviated from the known material sets to address underlying material stability and inter-layer reactions driven by temperature and pressure. The all-ceramic monolith pioneered by Saint-Gobain was produced by extruding and stacking alternating layers of anode and cathode materials separated by thin electrolyte and interconnect layers. This design used known and scalable manufacturing processes but still required manifold sealing on the sides of the stack to route reactants to and from the cells.

Tape-casting of anode or electrolyte supported cells, thermal spray coating onto metal supports, and extrusion and stacking of ceramic half-cells, all utilized known manufacturing methods adapted to the production of solid oxide cells. All three cell production methods strive to improve performance by thinning functional layers, reducing contact resistance, and reducing the number of high temperature firing steps. Whether planar, tubular, or monolithic, the stack design objectives remain a reduction of overall mass and volume, simplified sealing requirements, and lowered part count to reduce the overall system production cost. Azotera has pioneered a new approach using vanadia doped ceramic materials and a dry powder pressing additive manufacturing process (DPP-AM) to address these cell and stack production objectives.

DPP-AM addresses a number of these manufacturing and stack design weaknesses by producing high density monoliths with internal gas routing. Samples of YSZ produced via DPP-AM with a sintered area of 15 cm^2 and thickness of 2mm have been measured with a density exceeding 98.5% with sintering temperature of 1250°C. The process is amenable to a wide array of ceramic materials. The limitations of DPP-AM include the limited external geometry, currently simple polygons, the need for fine-grade ultra-dry powders, and the requirement for material co-sinterability when fabricating multi-compositional monoliths. While small internal structures such as channels can be formed without inducing cracking during sintering, the process can likely not form large hollow cavities. These limitations do not impede an all-zirconia based monolith for pressurized electrochemistry or various other process heating and heat exchanger applications.

A DPP-AM produced monolith provides increases the active area for reaction by producing ultra-fine microchannels. This 10x increase in area for the same material drives down cost.

Table 4. Summary of SOEC manufacturing pathways

Technology	Active Area per Unit Mass	Active Area per Unit Volume	Cost
Dip-coating tubular	400 cm^2/kg	500 cm^2/L	500 $/kW
Anode supported tape casting	350 cm^2/kg	1000 cm^2/L	400 $/kW
Metal support thermal spray	500 cm^2/kg	2,000 cm^2/L	200 $/kW
DPP-AM	5,000 cm^2/kg	20,000 cm^2/L	50 $/kW

Azotera's Monolith Manufacturing

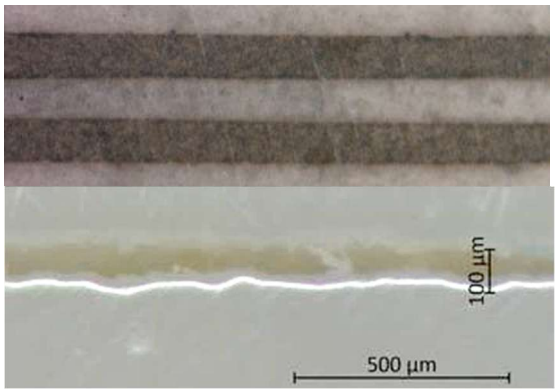

Figure 9. DPP-AM produced samples showing co-sintered layers and sub 100 micron channel

The DPP-AM fabrication process produces multi-compositional ceramic monoliths with internal gas routing formed through burnout of a fugitive material co-deposited with the functional ceramic layers. The prototype DPP-AM printer shown in Figure 10 has been demonstrated to produce uniform layers less than 20µm thick when sintered, can layer different functional materials into a single monolith, and produce uniform channels within those layers. Figure 9 shows examples of co-sintered YSZ and VYSZ, validating the co-firing of the electrode and electrolyte layers. Figure 9 also shows a contiguous sub 100 micron channel embedded in a dense YSZ sample, validating the fugitive material or lost wax process for forming these high surface area monoliths. The prototype DPP-AM device electrostatically deposits aerosolized powder onto a roller applicator, applies a prescribed pattern if necessary, then transfers powder to the build surface. After the layers have been sequentially added to the steel die, a hydraulic press compacts the layers into a 50% dense greenbody. During the sintering process a fugitive powder evaporates leaving behind high resolution internal gas routing within a fully dense zirconia structure. The internal flow routing eliminates costly and complex seals.

Five key capabilities distinguish DPP-AM from existing ceramic additive manufacturing methods: i) the processing applies to materials not amenable to laser sintering, ii) a single monolith can comprise interleaved layers of alternating materials, iii) materials incapable of pressureless sintering to full density can achieve high density, iv) a quality control step can reject a layer prior to adhering to prior layers, and v) co-deposition of fugitive material can form internal gas routing that eliminates costly and complex ceramic seals.

This ceramic manufacturing process enables this disruptive system design by fabricating monoliths with at least 10x the internal surface area of existing solid oxide stack designs. The high specific area intensifies the process and reduces mass 95% when compared to existing technology. The micro-channel ceramic monolith acts as a highly effective tube-cooled converter that lowers synthesis temperature and improves per pass conversion while recovering heat. The low mass system has a lower ultimate system cost and enables faster operational changes to match the dynamics of energy availability or pricing.

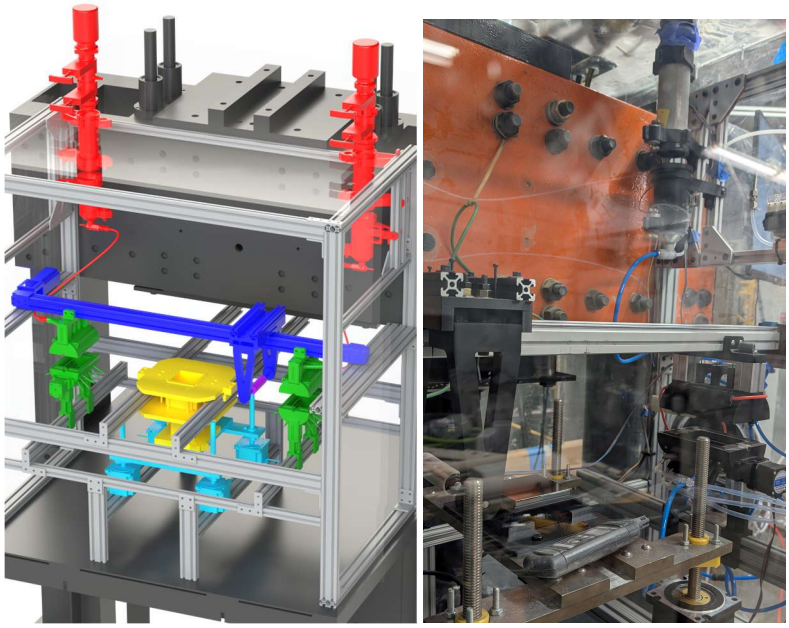

Figure 10. A 200T prototype DPP-AM comprises linear actuators (blue), a roller applicator (purple), dry powder dosing systems (red), powder deposition chambers (green), a split die system (yellow), and a fine movement plunger support (teal).

System Modeling

This section details how Azotera translates the benchtop validation measurements into system performance figures. Figure 11 depicts a system flow diagram with the thermo-mechanical elements, fluid flows, and energy inputs identified. The electrolyzer exhaust streams and the synthesis reactor heat the pressurized water before merging with a small quantity of recycled hydrogen to ensure reducing conditions. The oxygen product is vented and the hydrogen product is dried in a knockout stage and a desiccant bed before merging with the recycled gases in the ammonia synthesis loop. The pressure swing absorption beds separate fed by a large 150psi rotary compressor produce a stream of nitrogen and argon with less than 1000ppm oxygen. This nitrogen merges with the freshly made dry hydrogen and the recycle stream as the reactor feedstock. A high temperature and low temperature recuperator reduce the cooling and heating loads allowing the balance of the exothermic ammonia synthesis heat to pre-heat the electrolyzer water into steam. The reactor exhaust is cooled to -30°C to condense the ammonia. To avoid excessive inert buildup, a portion of the recycled volatiles are purged. The high pressure purge stream can be fed into the electrolyzer air electrode to reduce energy consumption.

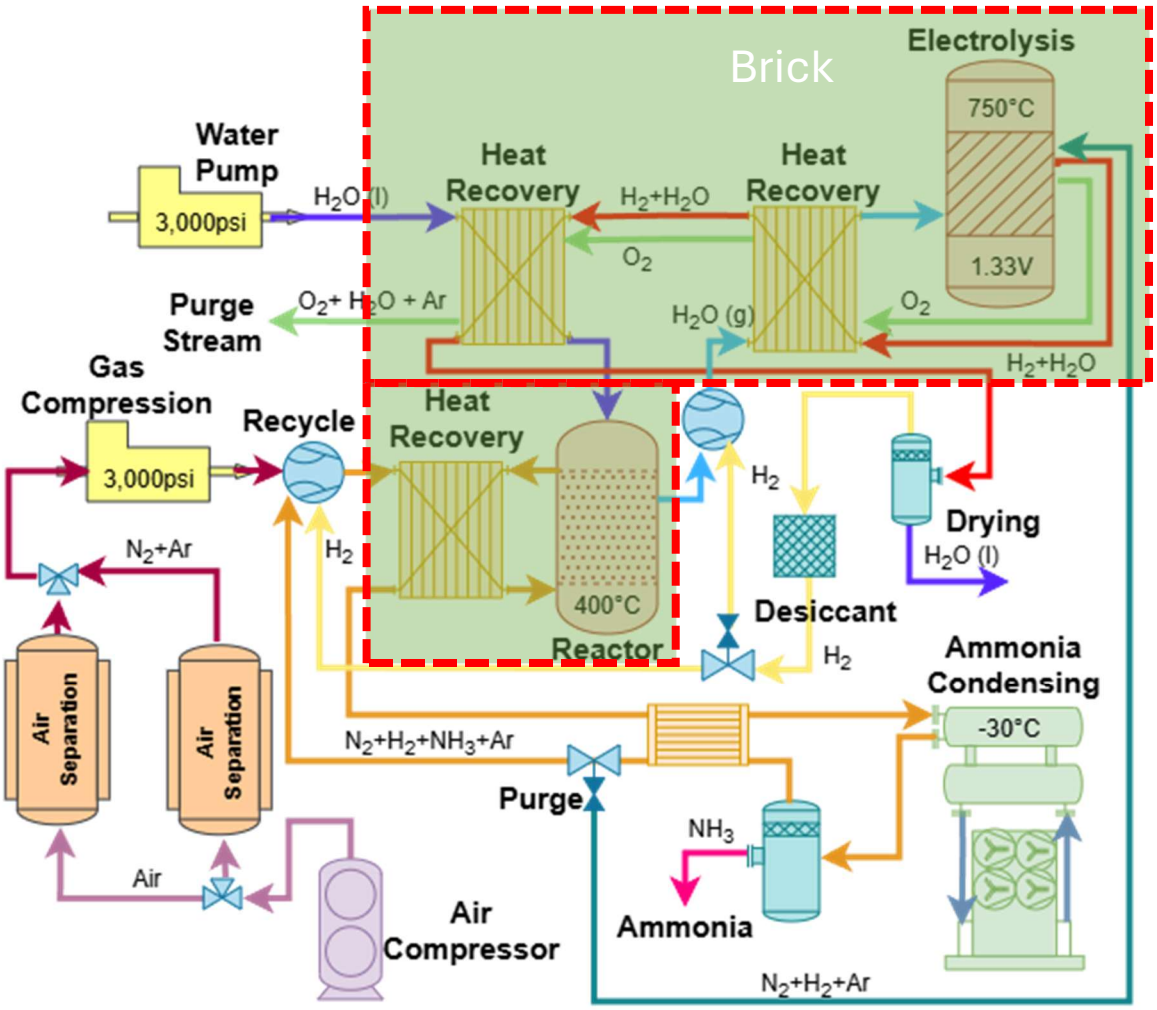

Figure 11 System flow diagram for an integrated high temperature electrolyzer and ammonia synthesis reactor

Feedwater Pumping: The feedwater compression assumes a pump efficiency of 85%, η_p, and a pump motor efficiency of 95%, η_m, based off existing boiler and feed pump technology. Equation (1) computes the pumping power in kW based on water density, ρ, pump and motor efficiencies, and differential pressure, $p_2 - p_1$. Equation (2) relates the hydrogen production rate, $\dot{m}_{12}$, in kg/s to the total current represented as the integral of the current density distribution, j, over the total active area of electrolysis. The molar mass of hydrogen, M_{H2}, and Faraday constant are 2.01588 g·mol^{-1} and 96,485 col·mol^{-1} respectively. Equation (3) computes the pumped water mass flow rate from the hydrogen production rate, the mass ratio of water and hydrogen, M_{H2O}/M_{H2}, and the recirculated water rate, $1/(1-X_{H2O})$ Recirculating the condensed exhaust water assumes an exhaust condenser can recover the water. This recovery is more viable at high pressure and higher exhaust humidity raising the condensation temperature and increasing system water utilization towards 100%.

$$\dot{W}_{pump} = \dot{m}_1 \cdot \frac{(P_2 - P_1)}{\rho \cdot \eta_p \cdot \eta_m} \quad (1)$$

$$\dot{m}_{12} = \frac{\int j \cdot \mathrm{d}A \cdot M_{H2}}{2 \cdot F} / 1000 \frac{\mathrm{g}}{\mathrm{kg}} \quad (2)$$

$$\dot{m}_1 = \frac{M_{H2O}}{M_{H2}} \cdot \frac{\dot{m}_{12}}{\left(1 - X_{H2O_8}\right)} \quad (3)$$

Steam Recirculating Ejector: The pumping pressure differential depends upon the motive fluid pressure requirement at the ejector inlet. Assuming small pressure ratios between the motive and entrained fluid, the compressibility of the gases can be neglected and the liquid-liquid jet pump formula of equations 4-9 applied. Equation (4) computes M, the mixing ratio between entrained and motive fluids based on the desired inlet and exhaust humidity. The steam electrode material may require a minimum or maximum humidification that determines the recirculation requirements. For example, a material may require between 25% and 62.5% humidity. The most efficient system recirculates the least water through the heat exchangers, thus implying the desired stack conditions would supply a mixture at 62.5% humidity and operate at 75% net utilization to produce a 25% exhaust concentration. This operation requires a 1:1 entrainment ratio in the ejector to ensure the humidity does not exceed 62.5% at the inlet. Increased entrainment lowers humidification at the inlet.

$$\mathrm{M} = \frac{\left(1 - X_{H2O_7}\right)}{\left(X_{H2O_7} - X_{H2O_8}\right)} \quad (4)$$

Equation (5) calculates C, the ratio of fluid densities between the entrained and motive fluids based on the exhaust humidity and assuming pure steam at the inlet.

$$\mathrm{C} = \frac{M_{H2} \cdot \left(1 - X_{H_2O_{in}}\right) + M_{H2O} \cdot X_{H2O_{in}}}{M_{H2O}} \quad (5)$$

Equation (6) describes N, the jet pump pressure ratio as the entrained flow pressure increase divided by the motive fluid pressure drop.

$$\mathrm{N} = \frac{(P_7 - P_8)}{(P_6 - P_7)} \quad (6)$$

Equation (9) computes this pressure ratio from the mixing ratio, the density ratio, four loss coefficients (K_m, K_d, K_s, and K_p), and R_d, the ratio of mixing tube to nozzle diameter as described in [51]. Two groupings of terms, G1 and G2 described by (7) and (8) simplify the formulation. Equation (10) defines ejector efficiency.

$$\mathrm{G1} = 2CM^2R_d^2/(1-R_d) \tag{7}$$

$$\mathrm{G2} = R_d^2(1+CM)(1+M)(1+K_m+K_d) \tag{8}$$

$$N = \frac{2R_d + \mathrm{G1}\left(1 - \frac{(1+K_s)}{(1-R_d)}\right) - \mathrm{G2}}{(1+K_P) - 2R_d - \mathrm{G1} + \mathrm{G2}} \tag{9}$$

$$\eta_e = M \cdot N \tag{10}$$

Ammonia Synthesis: Without the full-scale DPP-AM printer, it has not been possible to build sample microchannel reactors with sufficient activity to measure yields reaching 20%. The system performance estimates rely on a computationally efficient representation of real-gas effects suitable for high-pressure synthesis-loop modeling. Thermodynamic non-ideality in the synthesis-loop gas mixture is represented using Peng–Robinson (PR) mixture fugacity coefficients, which are used to form activities for (i) the equilibrium reference used in the approach-to-equilibrium metric and (ii) the activity-based driving-force terms in the reactor rate expression. The approach assumes: (i) a single vapor phase in the reactor operating envelope, (ii) no explicit association model for NH_3, and (iii) temperature- and composition-independent k_{ij} over the operating range. Synthesis reaction kinetics are governed by the local net ammonia formation rate per unit catalyst volume, $r(V)$ (e.g., $\mathrm{mol\,s^{-1}\,m_{cat}^{-3}}$). The functional form of this rate is the selected modified Temkin macro-kinetic correlation where $\alpha = 0.57$, $k(T)$ is the temperature-dependent rate coefficient, and A_{act} is a dimensionless lumped activity/effectiveness multiplier.

$$r = A_{\mathrm{act}}\, k(T) \left[K_{\mathrm{eq}}(T)^2\, a_{\mathrm{N_2}} \left(\frac{a_{\mathrm{H_2}}^3}{a_{\mathrm{NH_3}}^2} \right)^{\alpha} - \left(\frac{a_{\mathrm{NH_3}}^2}{a_{\mathrm{H_2}}^3} \right)^{1-\alpha} \right] \tag{11}$$

The temperature dependence is represented by an Arrhenius form with $\log_{10} k_0 = 14.7102$ and $E_a = 39057\ \mathrm{kcal\,kmol^{-1}}$ ($\approx 163.4\ \mathrm{kJ\,mol^{-1}}$). In this parameterization, R is expressed in $\mathrm{kcal\,(kmol \cdot K)^{-1}}$, T is in K, and k inherits the units of the underlying Temkin rate constant (e.g., $\mathrm{kmol_{NH_3}\,(h \cdot m^3)^{-1}}$). (Jorqueira et al. 2018).

$$k(T) = k_0 \exp\left(-\frac{E_a}{RT}\right) \tag{12}$$

The equilibrium constant is evaluated using the Gillespie–Beattie correlation (with T in K) (Gillespie and Beattie 1930).

$$\log_{10} K_{\mathrm{eq}} = -2.691122 \log_{10} T - 5.519265 \times 10^{-5}\, T + 1.848863 \times 10^{-7}\, T^2 + \frac{2001.6}{T} + 2.6899 \tag{13}$$

Ammonia Recovery: Ammonia is recovered downstream of the synthesis reactor by cooling the loop gas to a specified temperature, T_{sep}, at the loop pressure, P_{sep}. This simple condensing heat exchanger technology is well established. We model the separator as an equilibrium flash unit at $(T_{\mathrm{sep}}, P_{\mathrm{sep}})$, where NH_3 is the sole condensable species. N_2, H_2, and inert gases are treated as non-condensables and their dissolution in liquid NH_3 is neglected.

The model calculates the NH_3 "slip" (the unrecovered ammonia remaining in the vapor) based on a vapor–liquid equilibrium (VLE) constraint. The vapor composition is bounded by the saturation limit of ammonia at $(T_{\mathrm{sep}}, P_{\mathrm{sep}})$; any NH_3 exceeding this limit is removed as liquid. Pressure losses

across the separator are accounted for separately in the process model. Vapor–liquid equilibrium (VLE) is enforced by equating the fugacity of ammonia in the vapor and liquid phases.

The vapor-phase fugacity is defined by the real-gas mixture relationship where $y_{\mathrm{NH_3}}^{(v)}$ is the vapor mole fraction and $\phi_{\mathrm{NH_3}}$ is the mixture fugacity coefficient evaluated at separator conditions.

$$f_{\mathrm{NH_3}}^{(v)} = y_{\mathrm{NH_3}}^{(v)}\, \phi_{\mathrm{NH_3}}(T_{\mathrm{sep}}, P_{\mathrm{sep}}, \mathbf{y}^{(v)})\, P_{\mathrm{sep}} \tag{14}$$

The saturation limit is defined by the fugacity of the condensed liquid phase, $f_{\mathrm{NH_3}}^{\mathrm{sat}}(T_{\mathrm{sep}}, P_{\mathrm{sep}})$. We approximate this using the pure-component saturation pressure at T_{sep}, augmented by a Poynting correction to account for the compression of liquid NH_3 at high pressure:

$$f_{\mathrm{NH_3}}^{\mathrm{sat}}(T_{\mathrm{sep}}, P_{\mathrm{sep}})\& \approx P_{\mathrm{sat,NH_3}}(T_{\mathrm{sep}}) \times \exp\left[\frac{v_{\ell,\mathrm{NH_3}}}{RT_{\mathrm{sep}}}\left(P_{\mathrm{sep}} - P_{\mathrm{sat,NH_3}}(T_{\mathrm{sep}})\right)\right] \tag{15}$$

Equilibrium is enforced by setting $f_{\mathrm{NH_3}}^{(v)} = f_{\mathrm{NH_3}}^{\mathrm{sat}}$, yielding the saturation-limited vapor mole fraction.

$$y_{\mathrm{NH_3,slip}}^{(v)} = \frac{f_{\mathrm{NH_3}}^{\mathrm{sat}}(T_{\mathrm{sep}}, P_{\mathrm{sep}})}{\phi_{\mathrm{NH_3}}(T_{\mathrm{sep}}, P_{\mathrm{sep}}, \mathbf{y}^{(v)})\, P_{\mathrm{sep}}} \tag{16}$$

Electrolyzer: The electrolyzer represents the portion of the ceramic monolith separating oxygen from the incoming steam. Azotera is focused on an oxygen conducting YSZ electrolyte, but the balance of plant and reaction energy of equation (17) applies equally to a proton conducting cell in which the effluent stream would comprise hydrogen rather than oxygen. The same exhaust heat recovery possibilities exist, and only the de-humidification step would be redundant.

$$\Delta\bar{h}_{rxn} = \left(\bar{h}_{H_2}\langle T, P\rangle + 0.5 \cdot \bar{h}_{O_2}\langle T, P\rangle - \bar{h}_{H_2O}\langle T, P\rangle\right) \tag{17}$$

The total enthalpy of each reactant was determined as a function of both temperature and pressure using equation of state calculations for each fluid species according to the combination of enthalpy of formation and sensible energy change from the reference state as described in (18).

$$h_i\langle T, P\rangle = h_f\langle T_0, P_0\rangle + h_s\langle T, P\rangle - h_s\langle T_0, P_0\rangle \tag{18}$$

The operating voltage, V, determines both the electric power consumption, $\dot{W}_{elec}$, and the endothermic or exothermic nature of the electrochemical reaction. For a desired hydrogen production rate equation (2) can determine the total current necessary which is then multiplied by the operating voltage to compute the electrolysis power according to equation (19). Equation (20) computes the thermoneutral voltage, V_{th}, the operating condition at which the electrolysis will neither generate nor consume heat. If the operating voltage is above the thermoneutral voltage the electrochemistry generates usable heat.

$$\dot{W}_{elec} = V \cdot \int j \cdot \mathrm{d}A \tag{19}$$

$$V_{th} = \frac{\Delta\bar{h}_{rxn}}{2F} \tag{20}$$

Equation (22) computes the change in temperature between stack inlet and exhaust based on an energy balance consisting of the reaction enthalpy, Δh_{rxn} and the total electrical power. The

energy balance is divided by the heat capacity of the two reactant streams to determine the temperature change.

$$C_i = \left(1 - X_{H2O_i}\right) C_{p_{H2}} + X_{H2O_i} \cdot C_{p_{H2O}} \tag{21}$$

$$\Delta T = \frac{\dot{W}_{elec} - \dot{m}_{12} \cdot \Delta h_{rxn}}{(\dot{m}_7 C_7 + \dot{m}_8 C_8)/2 + \dot{m}_{14} C_{p_{O2}}/2} \tag{22}$$

The energy balance of (23) determines the ejector steam inlet temperature requirement, T_6. Equation (24) determines the exhaust recirculation fraction, R, from the inlet and exhaust humidity in a similar manner to how equation (4) found the mixing ratio, M.

$$R/M \cdot \bar{h}_{H2O}\langle T_6, P_6\rangle = R \cdot \bar{h}_8 - \bar{h}_7 \tag{23}$$

$$R = \frac{\left(1 - X_{H2O_7}\right)}{\left(1 - X_{H2O_8}\right)} \tag{24}$$

The hydrogen and steam mixtures at states 7 and 8 use the water concentration and equation (25) to determine the specific molar enthalpy.

$$\bar{h}_i = \left(1 - X_{H2O_i}\right) \cdot \bar{h}_{H2_i} + X_{H2O_7} \cdot \bar{h}_{H2O_i} \tag{25}$$

This analysis assumes an electrolyzer temperature of 700°C and constrains the inlet to outlet differential temperature to less than 100°C. Subtracting half of the temperature differential found in equation (22) from the operating temperature determines the stack inlet temperature, T_7, and adding half of the temperature differential determines the exhaust temperature, T_8.

The system level energy balance depends only on the electrolyzer voltage and operating to application pressure ratio, but the cost of the system depends on the ASR and system degradation. The current density distribution is determined from the operating voltage, V, the open-circuit voltage, V_{OCV}, and the ASR, according to equation (26). Equation (2) can then determine the total area required for a specific hydrogen production rate.

$$j = \frac{V - V_{OCV}}{\mathrm{ASR}} \tag{26}$$

The simplified model assumes an equipotential constraint across the electrode surface, but the open-circuit voltage varies according to the local reactant concentrations and the total pressure. Equation (27), known as the Nernst equation, describes the changing electrochemical potential of the reactants as the gas compositions, X_{H2O} and X_{H2}, change.

$$V_{OCV} = E^0 - \frac{R_u T}{2F} \cdot \ln\left(\frac{X_{H_2 0}}{X_{H_2} X_{O_2}^{0.5}}\right) \tag{27}$$

Equation (29) computes the reference voltage for the water-splitting reaction as a function of the operating temperature and pressure of the electrolysis where the entropy change is calculated with equation (28).

$$\Delta \bar{s}_{rxn} = \bar{s}_{H_2}\langle T, P\rangle + 0.5 \cdot \bar{s}_{O_2}\langle T, P\rangle - \bar{s}_{H_2O}\langle T, P\rangle \tag{28}$$

$$E^0 = \frac{\Delta \bar{g}_{rxn}}{2F} = V_{th} - \frac{T\{\Delta \bar{s}_{rxn}\}}{2F} \tag{29}$$

Component Sizing: Component volumes are scaled from the simulation basis to a target ammonia production rate using a linear scale factor f_{scale}, consistent with proportional scaling of flow-dependent hardware at fixed operating conditions.

The synthesis reactor is represented as a wall-coated microchannel monolith. The reactor-sizing routine returns an effective catalyst volume $V_{\mathrm{cat,solid}}$ (from the GHSV-based design step), which is then mapped to a physical monolith envelope volume by assuming that catalytic material exists only as a porous washcoat layer on the channel walls. Equating the catalyst solid volume to the washcoat solid volume gives an equation where $\varepsilon_{\mathrm{wc}}$ is the washcoat porosity, δ_{wc} is the washcoat thickness, and $S_{\mathrm{geo}} = A_{\mathrm{wall}}/V_{\mathrm{mon}}$ is the monolith wall-area density.

$$V_{\mathrm{cat,solid}} \;=\; (1-\varepsilon_{\mathrm{wc}})\,\delta_{\mathrm{wc}}\,A_{\mathrm{wall}} \;=\; (1-\varepsilon_{\mathrm{wc}})\,\delta_{\mathrm{wc}}\,S_{\mathrm{geo}}\,V_{\mathrm{mon}} \tag{30}$$

Solving for the monolith volume yields equation (31).

$$V_{\mathrm{mon}} \;=\; \frac{V_{\mathrm{cat,solid}}}{(1-\varepsilon_{\mathrm{wc}})\,\delta_{\mathrm{wc}}\,S_{\mathrm{geo}}} \tag{31}$$

The physical Haber–Bosch reactor volume reported by the sizing model is obtained by scaling the monolith volume to the target production rate and converting to liters, where V_{mon} is in m^3 and the factor of 1000 converts to liters. The sizing routine uses nominal washcoat/monolith parameters $\delta_{\mathrm{wc}} = 30\ \mu\mathrm{m}$, $\varepsilon_{\mathrm{wc}} = 0.50$, and $S_{\mathrm{geo}} = 10000\ \mathrm{m}^2/\mathrm{m}^3$.

$$V_{\mathrm{HB}} \;=\; (V_{\mathrm{mon}} \cdot 1000)\,f_{\mathrm{scale}} \tag{32}$$

The SOEC stack volume is determined from the total active cell area A_{cell} and an assumed active-area density ρ_{area}, which represents a compact planar stack envelope including interconnects, flow channels, and seals with $\rho_{\mathrm{area}} = 20{,}000\ \mathrm{cm}^2/\mathrm{L}$ used as the nominal value.

$$V_{\mathrm{SOEC}} \;=\; \frac{A_{\mathrm{cell}}}{\rho_{\mathrm{area}}}\,f_{\mathrm{scale}} \tag{33}$$

Heat exchangers are sized from their thermal duty using a single conservative volumetric power density ρ_Q applied uniformly to all exchanger services where Q_{peak} is the peak (maximum) duty across the voltage sweep, and negative duties are set to zero for sizing. A nominal value of $\rho_Q = 5\ \mathrm{kW/L}$ is used for all heat exchangers.

$$V_{\mathrm{HX}} \;=\; \frac{Q_{\mathrm{peak}}\,f_{\mathrm{scale}}}{\rho_Q} \tag{34}$$

Performance Estimation

A detailed design study varied operating conditions to identify the best system configuration. The performance validation tests will revise this analysis with updated measurements for the electrolyzer, heat exchanger, and ammonia reactor performance. Table 5 summarizes the operating condition assumptions and calculated parasitic losses for the primary balance-of-plant elements at a size-optimized design condition. The design condition operates above thermoneutral voltage to avoid any heating between states 5 and 6 and assumes a faradic efficiency of 97%. The analysis assumes a 94% efficient AC/DC rectifier, a pressure-swing-absorption nitrogen generator consuming 0.33 kWh/m^3 N2 for 99.9% pure nitrogen at 5 bar of which 1% is Ar. The nitrogen compressor is 85% efficient. A 2.5% purge from the synthesis loop keeps the inert buildup below 10% to maintain high ammonia yield. We assume a refrigerant condenser operating at -30°C at 33% of ideal efficiency, a coefficient of performance of 1.78. The resulting energy consumption of 7.39 MWh/ton represents a 40% reduction in energy consumption relative to state-of-the-art.

Table 5. Summary of performance calculations for a 2.5MW pressurized ammonia synthesis monolith system.

Input Parameters	Value	Units	Output Parameters	Value	Units
Power	2.5	MW	**Daily Energy Input**	60	MWh
AC/DC Rectifier	93	%	**H_2 Production**	1440	kg H_2/day
SOEC Voltage	1.30	V	**SOEC**	35.9	kWh/kg
Steam utilization	70%	%	**N_2 consumed**	6720	kg N_2/day
N_2 Production	3.0%	%	**N_2 gen Energy**	1774	kWh/day
N_2 Compression	1.5%	%	**N_2 Compression**	878	kWh/day
NH_3 Condensing	2.8%	%	**Condensing Refrigeration**	1679	kWh/day
Faradic efficiency	97.0%	%	**NH_3 Production**	7916	kg NH_3 /day
AR purge	3.0%	%	**Consumption**	7.58	MWh/ton
Refrigeration COP	1.78		**Efficiency**	68.2	%

Figure 12 illustrates some of the design tradeoffs that impact both size and efficiency. All of the cases from a multi-dimensional sensitivity plot are shown grouped by the operating voltage. The electrolyzer portion of the system is dictated by the area specific resistance (ASR) which relates the active area and current to the overpotential, e.g. the difference between operating voltage and open-circuit potential. The steam utilization and to a lesser extent temperature and pressure can impact the overpotential. At these operating conditions the open-circuit-voltage (OCV) is 1.15V. Temperature, pressure, materials, and membrane thickness can impact the ASR which is assumed to be 0.3 Ohm·cm^2. This results in a current density of 0.5A/cm2. At the design condition of 20,000 cm^2/L this results in a power density of 20kW/L.

The dominant driver of the ceramic reactor size vs. efficiency is the portion devoted to ammonia synthesis. A larger gas hourly space velocity (GSHV) increases single-pass yield and thus lowers the total flow through the reactor and associated heat exchanger. The analysis sizes the heat exchanger based on a constant 5kW/L, so as the reactor gets larger the incremental improvements in yield and reduced heat exchanger offset the reactor size until incremental yield improvements are small. Higher yield improves efficiency because less hydrogen is lost to purging out inert gases and the refrigeration load is lower. The optimum design uses a reactor section that is slightly larger than the size-optimal configuration to gain some efficiency benefit. The next section translates this performance dictated design into a manufacturing cost.

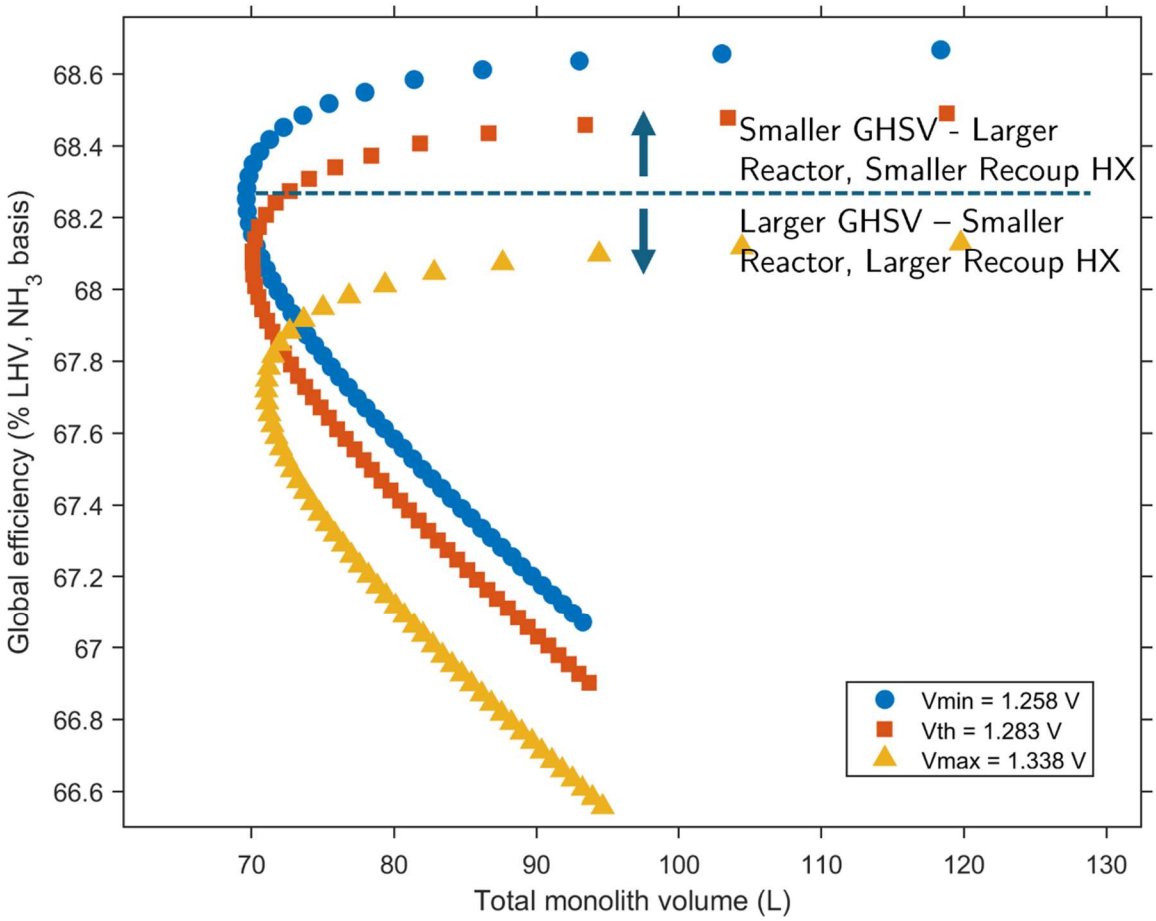

Figure 12. Modeling design study of integrated system identifies size-trade-offs with design conditions

Cost Estimation

The 50 $/kW cost estimate in Table 4 combines an estimate for the material production and the manufacturing cost using DPP-AM. Azotera has developed a printing cost target of 1 $/m^2 based on a rough bill of materials shown in Table 6 and the expected printing throughput. Azotera is validating the duration of each intermediate process step with the current DPP-AM prototype shown in Figure 10 to ensure the first full-scale printer prototype can demonstrate this production throughput. The bill of materials estimate for suggests a total cost range between $36k and $65k.

Table 6. DPP-AM printer bill of materials estimate

Item	Qty	Unit Cost ($)		Item	Qty	Unit Cost ($)	
		(high)	(low)			(high)	(Low)
Linear Actuators	14	1000	500	**Roller**	40	20	10
Solenoids	40	125	80	**Die Assembly**	2	4000	2000
Air Cylinders	120	25	10	**Die Lifter**	1	2000	1000
Hoses/barbs	250	1	0.5	**Dosing system**	10	100	50
Cascade	10	80	40	**Control box**	1	2000	1000
Chamber parts	20	60	20	**Vision QC system**	10	400	200
Carriage	10	50	25	**Air supply**	1	1000	500
Roller Transfer	3	600	300	**Filtration**	10	300	150
Enclosure	1	2000	800	**Assembly Labor**	200	75	55

Table 7 relates this CAPEX investment to a production cost of 1 $/m^2. Our initial throughput rate is targeting the deposition of a single 100 cm^2 layer every 10 s. At a 60% capacity factor this yields 19,000 m^2/yr. To achieve the target deposition cost the printer must reach this production speed while costing $50,000 and having less than $10,000 in annual maintenance over an 8-year lifespan. The time required for each roller application presents the largest uncertainty in this cost analysis. This deposition rate also impacts how many printers are required to produce the target volume of ceramic monoliths. Increasing the frequency of layer deposition is the priority of ongoing development work.

Table 7. Summary of DPP-AM production costs.

Assumptions	Value	Units	Output Parameters	Value	Units
DPP-AM printer cost	50,000	$	**Annual Mortgage**	9,372	$/yr
DPP-AM OPEX	10,000	$/yr	**DPP-AM annual cost**	19,372	$/yr
DPP-AM lifespan	8	yr			
Loan rate	10.0%	%			
Print Cross Section	100	cm^2			
Roll time	10	s	**Production Rate**	19,000	m^2/yr
DPP-AM capacity factor	60%	%	**Deposition Cost**	1.02	$/m^2

Table *8* details the production parameters for a single ceramic monolith used to estimate cost based on the 1 $/m^2 target for material deposition. The target geometry of 20,000 cm^2/L can be reached with channel heights of 50µm, solid layers of 12.6µm, and a channel area of 47.5%. The existing printer has demonstrated uniform coatings at the loading level necessary to achieve these thicknesses and the ability to create channels with this density of coverage.

The final geometry differs from the production geometry due to lateral shrinkage during sintering. The ratio of the green body and final density determines this shrinkage. The target monolith power and area specific power determine the number of electrolysis repeat units in the monolith. With feedback from validation tests, the system modeling provides a tool to determine the optimal ratio of heat exchange, reactor and electrolysis areas. Initial estimates, grounded in early experiments and known real-world performance of microchannel reactors, can project a 5:1 ratio of electrolyzer to reactor size and a 3:1 ratio for heat exchange. These ratios result in an 9" tall ceramic block producing 20kW.

This monolith would comprise 1,000 electrolysis cells, 875 heat exchange units and 525 reactor units. Each cell requires one interconnect, two channel, two electrode and one electrolyte layer while each reactor or heat exchanger layer requires a solid and a channel layer. Each layer can require either 3 or 4 deposition passes, one for each material in the layer. This totals nearly 30,000 roll passes, and at 10s per layer, this amounts to a 72+hr production time for each monolith. A production line producing 6,250 bricks per year (125MW/yr) would require one hundred printers.

Table 8. Summary of Gen 3 DPP-AM production parameters for a 20kW integrated monolith.

Assumptions	Value	Units	Output Parameters	Value	Units
Green body density	50%	%			
Final Density	98%	%	**Monolith Cross Section**	64	cm^2
Minimum Mass per coat	1	g	**Min layer thickness**	12.6	um
Maximum Mass per coat	4	g	**Max Layer thickness**	50.5	um
Channel Height	50	um	**Cell repeat unit height**	150	um
			HX/reactor repeat unit	62.6	um
Active Area Ratio	47.5	%	**Specific Active Area**	20,000	cm^2/L
Area Specific Power	0.65	W/cm^2			
Single Monolith Power	20	kW	**Number of Cells**	1015	units
Rolls per channel layer	4		**Monolith Height**	24.0	cm
Rolls per solid layer	3		**Number of rolls**	28,480	rolls
Electrolyzer: reactor size	5	ratio	**Deposition Area**	285	m^2
Electrolyzer: HX size	3	ratio	**Deposition Cost**	285	$/brick

This production cost can determine the monolith production cost given the geometry, the number of layers, the yield, and the material cost. The existing material cost at production rate < 1kg/day is exceedingly high: 500+ $/kg. Using lower cost material precursors, recovering ethanol and ammonia consumables and improved yield at scale, Azotera estimates a material production cost below 90 $/kg. This production cost assumes a 30 $/kg for feedstock materials, 6L of ethanol consumption per kg material, and 3 $/kg of energy costs. The final mass and the material waste factor determine the input material cost. Combining the material cost and the manufacturing cost arrives at a brick production cost of $994 which normalizes to 49.7 $/kW.

Table 9. Summary of Gen 3 DPP-AM production parameters for a 20kW integrated monolith.

Assumptions	Value	Units	Output Parameters	Value	Units
Monolith Mass	6.15	kg			
Solid Density	6	g/cm^3	**Monolith Volume**	1576	mL
Material Waste	20	%	**Material Input**	7.69	kg
Material Production Cost	100	$/kg	**Used Material Cost**	692	$/brick

Table *10* provides a summary of the 2.5MW system components that justify a 420 $/kW target. This represents a significant improvement over the state-of-the-art 400 $/kW stack and 1000 $/kW system cost. The balance-of-plant cost improvements stem from the elimination of compressors, heat exchangers and pre-conditioning systems. The dominant cost drivers include the pressure swing absorber system (PSA), the power electronics, the refrigeration system and the ammonia tank.

The controls and instrumentation cost estimates used known costs from Azotera's test equipment. The 22 ton storage tank cost includes the steel vessel, transport, and some of the connected safety valve and instrumentation. The PSA cost was extrapolated from commercial pricing of a fully turn-key 20m^3/hr system, roughly 1/10th the capacity needed. The 1,000 $/ton refrigeration cost only considers the compressor and condenser equipment since the evaporator would be part of the pressurized ammonia recovery units in the high-pressure cabinet. The power electronics only consider a MW-class AC-DC rectifier, and the two-way connection with a substation would need additional utility grade connection hardware. The site prep includes the groundwork for a 60'x60' pad with a simple steel structure to protect the equipment from weather. The transport assumed delivery to a local site, e.g. <500 mi, and the labor assumed 600 man hours at a loaded labor cost of $65/hr. Initial units would have higher labor costs, but Azotera envisions operating a lean production line producing one system per week with a dedicated 15-person staff.

Table 10. Summary of system component costs.

Assumptions	Value	Units	Output Parameters	Value	Units
System Size	2.5	MW	**NH_3 Tank**	0.75	$/L
Stack Production Cost	50	$/kW	**Water Tank**	0.25	$/L
Controls and Instruments	45,000	$/unit	**Tank size**	20	Days
High Pressure Cabinet	60,000	$/unit	**Tank Costs**	260,000	$
Pressure Swing Absorber	15,700	$/tpd	**Refrigeration**	1,000	$/ton
N_2 need	6.8	tpd/MW	**Refrigeration load**	12.7	ton
AC/DC Rectifier	60,000	$/MW	**Cooling Fans**	5,000	$/unit
Site Prep / Enclosure	50,000	$/unit	**Transport**	15,000	$/unit
Facility Overhead	20,000	$/unit	**Assembly/Labor**	39,000	$/unit
Total	1,049,984	$/Unit	**Scaled Cost**	420	$/kW

The equipment needed in a facility producing 50 ton/yr (200 kg/day) of high quality nanopowder would cost $4-$5 million. This consists of a $500k precipitation system, a $500k solids separation system, a $250k ethanol washing system and $1 million ethanol distillation and recovery system. The large spray dryer with nanopowder filtration system would add $1.5 million and a hazardous waste and water treatment system would add another $500k. At full capacity the nanopowder production consumables would add $1.75 million annually while producing enough powder to manufacture 6,250 bricks producing fifty 2.5MW systems totaling 125 MW/yr of capacity.

The operational costs would include the $1.75 million of material production consumables, labor and overhead of $4 million or more. The bulk of the operational cost would be purchasing the additional modular elements of each 2.5 MW system that total nearly $750,000. If the plant operated at capacity producing 50 systems per year, the operational costs would be over $40 million. The next section outlines the value in different market applications that justify a projected revenue potential of $250 - $500 million/yr from selling the 2.5MW ammonia plants with 80%-90% gross margin.

Summary System Model

A simple block diagram highlights flows between components, cost, and energy consumed.

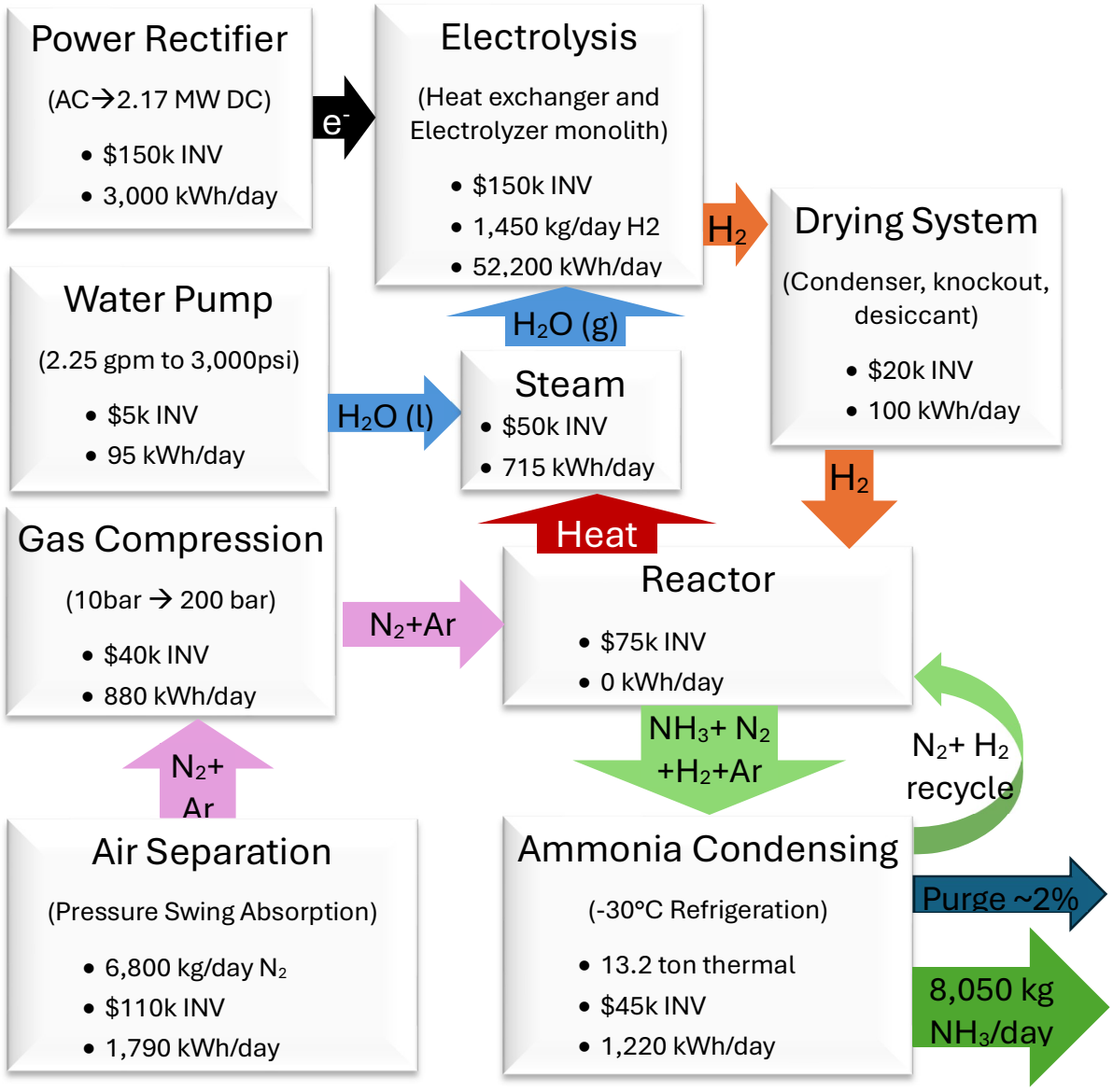

Figure 13. Block diagram of Azotera ammonia production with approximate costs and energy consumption

Table 11. Summary Energy Balance Producing 8ton/day from 60MWh (7.5MWh/ton ~70%)

Component	Energy Consumed (kWh/day)	Cost ($1,000's)	Component	Energy Consumed (kWh/day)	Cost ($1,000's)
Power Rectifier	3,000	150	**Drying**	100	20
Electrolysis	52,200	150	**Steam**	715	50
Water Pump	95	5	**Reactor**	0	75
Gas Compresor	880	40	**Condenser**	1,220	45
Air Separation	1,790	110	**Total**	60,000 (24hrx2.5MW)	$645,000

Market Opportunity Analysis

On-Farm Anhydrous Production / on-site Industrial Ammonia: This use case represents the single-direction electrolysis plant that will validate the operational efficiency and flexibility of Azotera 's system. The scenario utilizes grid-connected or grid-independent energy production from wind, solar, or hydro to power Azotera's ammonia bricks through a simple rectifier. This system has the lowest cost balance-of-plant surrounding the Azotera brick. This simple analysis varies the installed renewable cost and operating capacity factor to project the net ammonia production, unit cost, and simple payback period. A 2.5MW system purchased at 1,000 $/kW or $2.5 million (60% gross margin). Combined with a solar or wind installation ranging from 0.50 $/W – 1.0 $/W ($1.25M - $2.5M). This analysis shows that even low-capacity factor installations can save farmers money and installations with at least a 25% capacity factor can compete with wholesale anhydrous prices. The payback period, including maintenance costs, of 5-8 years is a great value for farmers.

Input Assumptions

System Nameplate	2.5	MW
Energy Consumption	7.5	MWh/ton
Ammonia System CAPEX	1,000	$/kW
Lifespan	20	Yrs
Renewable O&M	0.01	$/W-yr
Ammonia System O&M	25	$/kW-yr
Finance / Loan Rate	8%	%

Table 12. Effective Ammonia production cost in $/ton for grid-independent operations

Installed Renewable Cost ($/W) \ *Operating Capacity Factor*	15.0%	17.5%	20.0%	22.5%	25.0%	27.5%	30.0%	32.5%	35.0%	37.5%	40.0%
0.50	579	496	434	386	347	316	289	267	248	231	217
0.55	608	521	456	405	365	332	304	281	260	243	228
0.60	637	546	478	425	382	347	318	294	273	255	239
0.65	666	571	499	444	400	363	333	307	285	266	250
0.70	695	596	521	463	417	379	347	321	298	278	261
0.75	724	621	543	483	434	395	362	334	310	290	272
0.80	753	646	565	502	452	411	377	348	323	301	282
0.85	782	670	587	521	469	427	391	361	335	313	293
0.90	811	695	608	541	487	442	406	374	348	324	304
0.95	840	720	630	560	504	458	420	388	360	336	315
1.00	869	745	652	580	522	474	435	401	373	348	326
Production (ton/yr)	**438**	**511**	**584**	**657**	**730**	**803**	**876**	**949**	**1022**	**1095**	**1168**

Table 13. Simple payback period for on-farm anhydrous ammonia production

Ammonia Sale Price ($/t)	15.0%	17.5%	20.0%	22.5%	25.0%	27.5%	30.0%	32.5%	35.0%	37.5%	40.0%
600	21.4	17.1	14.3	12.2	10.7	9.5	8.6	7.8	7.1	6.6	6.1
650	19.7	15.8	13.3	11.4	10.0	8.9	8.0	7.3	6.7	6.2	5.8
700	18.3	14.8	12.4	10.7	9.4	8.4	7.6	6.9	6.4	5.9	5.5
750	17.1	13.9	11.8	10.2	9.0	8.0	7.2	6.6	6.1	5.6	5.2
800	16.2	13.2	11.2	9.7	8.6	7.7	6.9	6.3	5.8	5.4	5.0
850	15.4	12.6	10.7	9.3	8.2	7.4	6.7	6.1	5.6	5.2	4.8
900	14.7	12.1	10.3	8.9	7.9	7.1	6.4	5.9	5.4	5.0	4.7
950	14.1	11.6	9.9	8.6	7.6	6.8	6.2	5.7	5.2	4.9	4.5
1000	13.6	11.2	9.6	8.3	7.4	6.6	6.0	5.5	5.1	4.7	4.4
1050	13.1	10.9	9.3	8.1	7.2	6.5	5.9	5.4	4.9	4.6	4.3

Utility Backup and Anhydrous Offtake: This uses case represents the greatest value scenario and can thus command the highest sale price. When Azotera demonstrates durability through the pilots, utilities and regulators have a multitude of reasons to adopt this technology:

1) The system provides backup power at congested substations for days/weeks
2) The system provides dispatchable load that can be shed during peak periods
3) The system creates alternative revenue through ammonia offtake
4) The system increases the use of intermittent green power to improve regulatory compliance
5) The system reduces cost and increases the reliability of fertilizer supplies for local farmers
6) The system reduces carbon emissions from the ag sector, as much as 660,000 t/yr in WA

The simple analysis relies on wholesale energy price data shown in Figure 14.

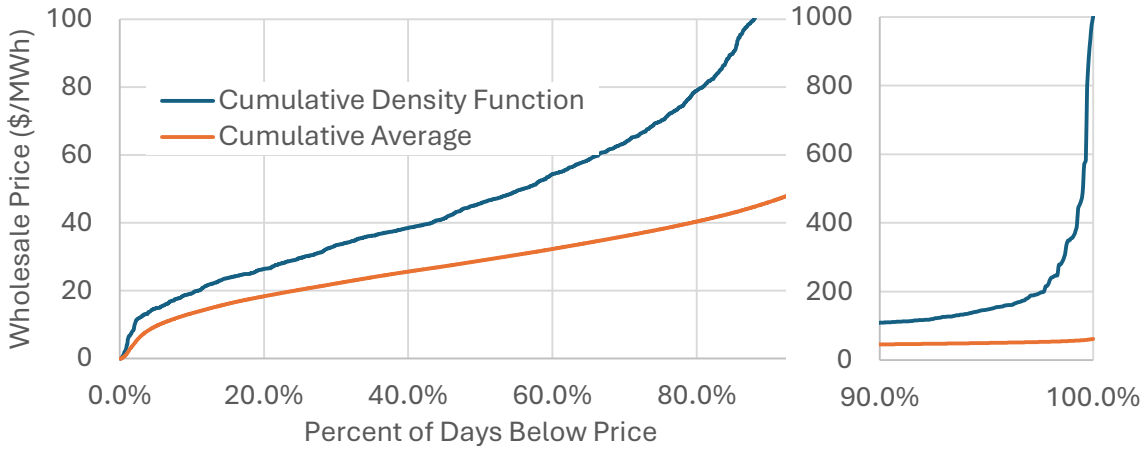

Figure 14 Mid Columbia Wholesale Energy Prices 2020-2025 ($/MWh)

Table 14 shows the calculated net present value of the 2.5MW system using an 8% discount factor and several assumptions:

- System operates as a 2.5MW generator 500 hr/yr
- Net round-trip efficiency is 50%
- When generating power it displaces fossil generation, mitigating a 100 $/MWh CETA compliance cost
- System receives 50 $/ton carbon credit at a rate of 2.4 ton Co2 per ton NH3
- System is valued at $1M/MW for the reliability aspect of the installation

Table 14. Net Present Value ($Million) of 2.5MW reversible Ammonia System with 360 hr storage

Ammonia Production (hr/yr) \ Contracted Ammonia Offtake ($/ton)	350	400	450	500	550	600	650	700	750
4,000	$8.33	$8.82	$9.31	$ 9.80	$10.29	$10.78	$11.27	$11.76	$12.25
4,500	$8.55	$9.12	$9.69	$10.27	$10.84	$11.41	$11.98	$12.56	$13.13
5,000	$8.72	$9.38	$10.03	$10.68	$11.34	$11.99	$12.65	$13.30	$13.96
5,500	$8.83	$9.56	$10.30	$11.04	$11.77	$12.51	$13.25	$13.98	$14.72
6,000	$8.87	$9.69	$10.50	$11.32	$12.14	$12.96	$13.78	$14.59	$15.41
6,500	$8.83	$9.73	$10.63	$11.53	$12.43	$13.33	$14.23	$15.13	$16.03
7,000	$8.70	$9.68	$10.66	$11.64	$12.63	$13.61	$14.59	$15.57	$16.55
7,500	$8.44	$9.50	$10.56	$11.63	$12.69	$13.75	$14.82	$15.88	$16.94
8,000	$ 7.94	$9.08	$10.23	$11.37	$12.52	$13.66	$14.81	$15.96	$17.10

Renewable Energy Firming: This use case represents a behind-the-meter installation at a renewable energy farm used for turning an intermittent energy source into a dispatchable power plant with seasonal energy storage. The generation coincidence of solar that created the well-known duck-curve, and the seasonality of wind means these low-cost energy sources sell into the market at the same time, occasionally driving wholesale prices negative. This market dynamic makes low capacity factor installations financially unviable. Shifting solar energy a few hours to the 'shoulder' periods represents a great use case for batteries, e.g. daily operation and storing 2-4 hours. This can improve project economics marginally. Examination of wholesale prices can identify some daily periodic behavior driven by the interaction between the solar production cycle and consumer demand curve. However, most price variation occurs over weeks and months in response to seasonal changes in energy use, e.g. heating and air conditioning, and seasonal variation in hydropower and wind energy. No battery system can provide energy firming over these time scales to capture the more valuable seasonal energy arbitrage case. A solar installation that produces power 25% of the time, coincident with the lowest daily wholesale prices, could increase revenue 500% by shifting that energy to the 15% of time with the highest wholesale prices. The revenue increases despite a 50% energy loss from the round-trip operations.

The analysis can use the same assumptions for energy efficiency and maintenance costs as before and calculate the additional value to a renewable energy farm. Investors in these infrastructure projects typically expect high rates of return. The utilities demand for firm dispatchable power could permit conversion of existing energy farms from intermittent generators to dispatchable power as well as accelerate approvals of new installations. Table 15 quantifies the value of the ammonia system to the energy farm expressed in multiples of the assumed 500 $/kW COGS. You can see the value increases with capacity factor and decreases with the required investor return. This scenario is slightly less valuable that the utility backup scenario, but is not dependent on ammonia offtake. This represents a 10x to 50x larger market in terms of capacity.

Table 15. Net Present Value ($Million) of a 2.5MW Nameplate System Used to Firm Renewable Power

Capacity Factor \ Investor Internal Rate of Return (%)	7%	8%	9%	10%	11%	12%	13%	14%	15%
20.0%	$ 5.21	$ 4.77	$ 4.38	$ 4.05	$ 3.75	$ 3.48	$ 3.24	$ 3.03	$ 2.83
22.5%	$ 5.51	$ 5.05	$ 4.64	$ 4.28	$ 3.96	$ 3.68	$ 3.43	$ 3.20	$ 3.00
25.0%	$ 5.78	$ 5.30	$ 4.87	$ 4.49	$ 4.16	$ 3.86	$ 3.60	$ 3.36	$ 3.15
27.5%	$ 6.03	$ 5.52	$ 5.08	$ 4.68	$ 4.34	$ 4.03	$ 3.75	$ 3.50	$ 3.28
30.0%	$ 6.26	$ 5.73	$ 5.27	$ 4.86	$ 4.50	$ 4.18	$ 3.89	$ 3.64	$ 3.41
32.5%	$ 6.44	$ 5.90	$ 5.42	$ 5.00	$ 4.63	$ 4.30	$ 4.01	$ 3.74	$ 3.51
35.0%	$ 6.59	$ 6.04	$ 5.55	$ 5.12	$ 4.74	$ 4.40	$ 4.10	$ 3.83	$ 3.59
37.5%	$ 6.72	$ 6.16	$ 5.66	$ 5.22	$ 4.83	$ 4.49	$ 4.18	$ 3.91	$ 3.66
40.0%	$6.83	$ 6.26	$ 5.76	$ 5.31	$ 4.92	$ 4.57	$ 4.25	$ 3.97	$ 3.72
42.5%	$ 6.93	$ 6.35	$ 5.84	$ 5.39	$ 4.99	$ 4.63	$ 4.31	$ 4.03	$ 3.77
45.0%	$ 7.01	$ 6.42	$ 5.90	$ 5.45	$ 5.04	$ 4.68	$ 4.36	$ 4.07	$ 3.82

Azotera's Scale-up Technical Risks

Energy system research carries technological and business risks which can be mitigated by an experienced team and an adaptable concept. The crucial elements for cost-effective performance include high internal surface area, mechanical strength and robustness to temperature variations, and sufficient catalytic activity for ammonia synthesis and decomposition. The risks include:

1) Challenges with economically manufacturing ultra-high surface area monoliths
2) Challenges with ceramic fracture during sintering, heat up or operation
3) Challenges with sufficient catalytic activity for synthesis or decomposition
4) Challenges with durability or system flexibility to operate intermittently.
5) Challenges with the business model or financing deployments.
6) Challenges with safety of pressurized fluids, high voltage and hazardous materials

Azotera has systematically worked to address these risks through proof-of-concept demonstrations, simultaneous pursuit of alternative strategies, and modular designs. Table 16 summarizes specific technology development risks detailed in this section.

Table 16. Risk identification and management summary

Risk	Likelihood Severity	Mitigation measures	Contingency measures
Nanopowder material production cost	Unlikely Minor	Transition to low-cost precursors, recover ethanol	Evaluate flame pyrolysis with industrial partners
Additive ceramic printing cost	Possible Moderate	Continuous roller deposition, scale-up of cross section area	Production scale and offset with with BoP savings
Ceramic fracture during sintering	Unlikely Moderate	Improve deposition uniformity through calibrating deposition	Periodically print a levelling layer
Ceramic fracture during operation	Likely Moderate	Print insulative layers with unconnected gas pockets	Hot ceramic joint connection between separated monoliths
Ceramic fracture during heat up	Possible Minor	Reduce the applied heating rate	Pass nichrome heating wire through open channels
Ceramic fracture from fluid pressure	Possible Significant	Reduce channel sizes, thicken the outer dense shell, and sinter denser	Use a pressure vessel to reduce relative environmental pressure
Ceramic fracture during fuel cell mode	Possible Severe	Alter flow path to predominately counter-flow, increase air flow	Create an ancillary thermal management fluid circuit
Crossover leakage exceeds threshold	Likely Significant	Print thicker membranes and sinter to higher density	Apply impregnation techniques to fill residual porosity
Insufficient ammonia production	Possible Moderate	Reduce flow rate and increase pressure	Test higher performance catalysts
Insufficient ammonia decomposition	Unlikely Moderate	Raise operating temperature	Add Iron or Nickel catalyst
Insufficient catalyst durability	Possible Minor	Use higher purity nitrogen feedstock	Use different catalyst
Limited turndown capacity	Possible Minor	Sequence multiple monoliths to form overlapping operating bands	Analyse a battery hybrid system to expand the operation
Performance durability / life cycle	Possible Moderate	Reduce severity of operating conditions (pressure/temperature)	Use separate systems for electrolysis and fuel cell modes
Off take contracts below wholesale	Possible Moderate	Ensure initial contract length covers payback period	Wholesale pricing on spot price market or build large storage
Unforeseen permitting / regulatory costs	Unlikely Moderate	Use known equipment for ammonia handling and power connection	Operate fully grid disconnected
Excessively expensive project financing	Possible Significant	Create operating history with pilot deployments	Secure firm long-term offtake contracts

Production Cost Risks: The four drivers of installed cost are: i) input materials for nanopowder synthesis, ii) cost of additive ceramic printing equipment, iii) cost of system balance-of-plant equipment and assembly, and iv) cost of site preparation and installation.

Materials Cost: The integrated high pressure monolith eliminates 95% of the material mass for a similar solid oxide system. Despite this, the material cost is a primary driver of the brick production cost. Azotera has developed a scalable nanopowder production process that has shrunk the labor cost and reduced waste, lowering material cost from approximately 1500 $/kg at the lab scale to 500 $/kg at the proof-of-concept scale. Without significant changes, this system could scale to under 250 $/kg. Further cost reductions planned for 2026 will apply basic chemical engineering to produce the same grade product from lower cost precursors with the aim to reach a target material cost of 100 $/kg. This will yield a net contribution under 35 $/kW of the installed system cost.

Printing Cost: 2026 development tasks are focused on de-risking this production cost by scaling the additive manufacturing and reaching a reliable throughput that results in an amortized cost of under 1 $/m^2 deposited. The proof-of-concept printer has demonstrated the individual functional elements and the design for a continuous roller system is complete. Fabricating this dual gantry continuous belt DPP-AM printer is critical to reaching the target production cost of under 20 $/kW. 2027 will focus on reliability and uptime improvements to extend equipment lifetime so that a $50k to $100k printer can last long enough to reach the amortized 1 $/m2 target.

System Cost: The balance-of-plant relies on off-the-shelf TRL9 equipment (on a technical readiness level scale of 1-9, where 9 it the highest). A detailed consumer reports type bill of materials (BOM) study will evaluate the cost, performance, and reliability tradeoffs with different equipment suppliers. A combination of known suppliers could reach the estimated system cost of 200 $/kW for a non-grid connected installation. Additional supplier sourcing and further deconstruction of modular elements into sub-component costs could yield additional savings.

Site Costs: The specific site preparation costs will depend on the climate, surrounding built environment, and possible connection to a utility. Bi-directional utility connection will be product use case dependent and could add 50%-100% to the installed system cost.

Ceramic Fracture Risks: Economical production requires ceramic monoliths scale-up to 500mL.

During Sintering: This risk pertains to challenges with matching sintering profiles of different materials and uniform shrinkage across the cross-section during the high-temperature firing of larger ceramic monoliths. Avoiding fracture requires a sufficiently uniform pressed green body density using materials with sufficiently similar sintering behavior to avoid strain during densification. Azotera has met this materials and manufacturing challenge with button cells that have shown the material compatibility. When the powders were prepared via the same production method and the compositions all reached the cubic phase at similar temperatures, the samples came out uniform and flat. In these sample preparations the powder was leveled in the 25mm die via acoustic resonance vibration. The production version uses a powder coating and roller system to create patterned layers. Achieving uniform density relies on uniform coverage of the powder coating process and correct alignment of the interwoven patterns. The team has developed a powder coating system with multiple charge points and fully turbulent and distributed powder injection to create coating that have been measured to be within +-2% of average across the length of the roller applicator. Production of samples larger than 50mL and with cross sections greater than 25 cm2 will be necessary to validate if this is sufficiently uniform. If samples fracture during sintering there are several strategies for firing schedules, powder particle size distribution

adjustments, and sintering aids that can align the densification of each layer. If the samples are clearly lower density near the edges due to bias in the coating chamber or pressing, then periodic leveling layers can be printed to compensate for the bias.

During Operation: This risk identifies ceramic stress/strain caused by temperature gradients during operation that could cause failure. In the preferred implementation that avoids high temperature seals, the synthesis section at 350 °C - 450°C is immediately adjacent to the electrolysis section at 650 °C - 750°C. The design may require thermal spacing layers which serve only to provide a more gradual temperature transition in the vertical orientation of the ceramic. This may add as much as 10% to the brick manufacturing cost. An alternative implementation separates the synthesis and heat exchanger portions into separate ceramic monoliths and employs a hot gas connection. This brings a separate set of material and compression challenges, but would allow each brick to operate in a narrow temperature window.

During Heat Up: One advantage of ceramics in microchannel heat exchanger applications is the low thermal conductivity through the solid which allows for high effectiveness in short lengths. This may limit the rate of heating from room temperature to operating conditions if severe temperature gradients cause structural failures. Testing will determine the bounds for heating and cooling bricks. This will influence the operations schedule and potentially the size of a battery system used for black start capability.

Fluid Pressure: A unique aspect of the microchannel design is the ability of the ceramic brick to function as the pressure containment vessel. The ceramic experiences differential pressure in two places, i) between the ambient environment and the internal channels, and ii) between the fuel and oxidant channels across the thin tri-layer membrane. The size of the channels, the effective porosity of the brick, and the density of the shell layer will impact the shell thickness requirement and thus the cost of each brick. The width of the fluid channels and the differential pressure control of the back-pressure regulators will impact the required thickness of the electrochemical tri-layer. A thinner tri-layer improves performance and wider channels relative to walls increases reactant area and performance. This is an area where improved manufacturing precision, e.g. smaller feature widths, will allow for thinner membranes and higher performance for a specified pressure differential tolerance. Manufacturing improvements become performance improvements.

Fuel Cell Mode Operation: A unique advantage of solid oxide electrolysis is the ability to operate at or near the thermoneutral voltage. This limits the local heat production in the electrolysis section, reducing temperature gradients. In fuel cell operation, local heat production is unavoidable. Typically, the thermal gradients are handled with excess air flow, but at high pressure this would entail excessive parasitic losses from air compression. During periods of power generation, Azotera intends to produce a concentrated oxygen stream using the air separation system that nominally produces nitrogen for ammonia synthesis. This decreases the compressed mass flow 95% and raises the operating voltage and thus efficiency of the power production. Some of the excess heat can be recovered into the decomposition of ammonia into hydrogen, but if this proves insufficient to mitigate overheating or fracture, the design would require a secondary fluid for thermal management. A closed-loop circuit running a supercritical CO2 cycle would efficiently recover this waste heat as additional power. This implementation would set the minimum operating capacity in fuel cell mode based on the turn-down capacity of this rotating equipment.

Crossover Leakage: The faradic efficiency of any electrochemical membrane is critical to overall system performance. Performance and efficiency degrade if electrons or mass that is not the

intended ion, $O^{=}$, can leak across the electrochemical tri-layer. With the selected material, electron leakage is not a concern. Mass leakage would likely occur through pinholes; defects in the production that leak oxidant back into the fuel channels. Making thinner tri-layer samples increases performance by lowering ohmic resistance, but also increases the likelihood of these pinholes forming. If a reduction to 10um layers doubled performance, thus halving cost, Azotera might tolerate having a 0.5% leakage that caused a 1% loss in efficiency. This risk represents a managed tradeoff in performance and efficiency. As manufacturing improves uniformity of the applied powder coating layer, then thinner layers would be possible without any or with an acceptable quantity of pinholes.

Ammonia Conversion: The conversion between hydrogen + nitrogen and ammonia occurs at catalyst sites when the reactants are at high temperature and pressure. The equilibrium conditions are known precisely from theory, the catalytic activity can be accurately measured in the lab, but it is impossible to perfectly predict the achievable yield in a full-scale reactor.

Ammonia Synthesis: The various commercial implementations from Topsoe, Thyseenkrupp, Linde, and Casale for producing anhydrous ammonia differ primarily in the physical structure and operating conditions of the ammonia synthesis loop. Each manufacturer has optimized temperature, pressure, and recycle conditions for a specific catalyst material and support structure. Examples with iron catalyst supported on zirconium oxide in a porous microchannel reactor, akin to the channels within Azotera's bricks, have guided an initial design point and performance expectations. The performance depends on the residence time, surface features, catalyst particle size, space velocity, temperature, pressure, and heat transfer from the reaction sites. Mitigating the risk prior to testing would be less cost effective than adapting to the measured performance with changes in size, operating conditions, or catalyst material. Initial estimates place the optimum reactor size at nearly 20% of the total volume. If measured performance falls short 50%, this could add as much as 20% to the cost of the monolith or 4% to the CAPEX of the system.

Ammonia Decomposition: Ammonia cracking has become a topic of considerable engineering focus as companies looking to import hydrogen via more transportable ammonia work to improve the efficiency of decomposing ammonia and separating out a 99.999% pure hydrogen stream. The decomposition is endothermic, requiring heat. By incorporating directly into the ceramic monolith in the same fashion as the ammonia synthesis, the exothermic fuel cell operation provides this heat. The identified risk represents an underestimate of the required catalyst area required to reform the ammonia. An adjustment to the operating conditions, e.g. higher temperature, represents the most straightforward solution to this risk.

Turndown Capacity: The ability to operate at reduced output represents the final design and operational risk identified. The technical background portion of section 4 showed the narrow operating band within which the thermoneutral operation can be maintained. This typically creates a 2:1 turndown capacity. There are operation strategies to widen this window from 2:1 and create 5:1 or even 8:1 turndown capacity. Additionally, the modules can be sequenced in their operation to create a higher plant turn-down capacity. If the fuel cell operations require the additional thermal management circuit, that same circuit could be used to increase operating voltage and turndown capacity in electrolysis operations.

Equipment Durability and Lifespan: The economics of the system depend on the durability of the equipment. The balance-of-plant electronics, fans, and membranes are designed for 20+ year service life. Azotera has tested the materials for hundreds of hours, but long term durability tests of the monoliths will not begin until late 2026. The primary drivers of electrolysis and catalyst

degradation are temperature, current, contamination, and redox or thermal cycles. These stressors can be mitigated through design and operation. Some bounds on lifespan can be estimated from lab tests and similar products, but the extreme pressure conditions introduce new uncertainty. Azotera is targeting the DOE benchmark of degradation less than 0.4% per 1,000 hours which would reduce output to 75% after 7 years. Since the monolith comprises 20% of the system cost, high degradation can be managed with periodic stack replacements. Two stack replacements increase CAPEX cost 40% to reach the 20 year plant lifespan. Additional materials development and operations experience could extend lifespan further.

Offtake Contracts: To ensure profitability of each installation, including the pilots, Azotera seeks to secure firm off take contracts for at least the duration of the payback period. Azotera is evaluating the market acceptance for fixed-price vs spot price purchases of anhydrous ammonia. Presently the distributors apply a markup and pass on any price volatility from the global energy markets onto their consumers. Azotera will investigate working closely with value-added fertilizer firms that add nutrients and produce other fertilizer products from anhydrous ammonia, as these mid-stream suppliers may value diversifying some purchases away from the primary producers. Higher offtake rates shorten payback, and high enough rates from a green premium would allow for contracts of just 2-3 years. If Azotera cannot secure firm offtake contracts at or above market rates, Azotera would be subject to the price volatility of the primary ammonia producers, adding significant uncertainty to the payback period of the system.

Permits and Regulatory Risks: This is generally seen as an area of strength for the proposed technology because the modular behind-the-meter concept faces fewer regulatory and permit risks than technologies producing hydrogen and relying on customer connection to the utility grid. Keeping units below 20MW (50 tpd) reduces the reviews necessary for grid connection and accelerates permitting. The low flammability of anhydrous and internal conversion of the produced hydrogen reduces permitting requirements relative to facilities with substantial hydrogen flows or storage. The regulatory environment, particularly rate boards for utilities would likely support the additional resiliency of a reversible load and the ancillary carbon reduction for food production. The system benefits from any regulatory hurdles or costs added to fossil-derived ammonia production, e.g. a border emissions tax.

Financing Risks: Limited operational history poses a significant financing/insurance risk. Azotera intends to pursue concurrent pilot demonstrations with multiple utilities while running accelerated lifecycle testing of the monoloiths and balance-of-plant systems to establish best-practices, maintenance schedules including possible monolith/brick change out schedules. The focus of these operations examples is to reduce the financing risk and demonstrate infrastructure grade equipment reliability. In most cases of utility infrastructure upgrades, the publicly owned or investor owned utilities bring their own financing. For the expanded energy storage market at data centers or wind/solar farms the individual project financing risk can be outsourced to established project developers. Renewable project developers tolerate the grid interconnection delays because it comes with a guaranteed off-taker for the electric power. The limited hydrogen infrastructure has presented a challenge for developers to secure 20 year off-take contracts in hydrogen production. Because Azotera A produces a readily stored, sold, and transported commodity product, the loss of a primary off taker is less damaging to the project economics, making financing easier.

Safety Risk Management: Azotera's technology incorporates high-pressure fluid circuits, on-site ammonia synthesis and storage, and high-voltage electrochemical systems. These factors introduce inherent safety risks that must be systematically managed. The three pillars of Azotera's

safety culture are i) adherence to established engineering standards, ii) robust engineered controls, and iii) formalized operating procedures. The goal is to achieve utility-grade reliability and exceed applicable regulatory requirements.

Azotera adheres to internationally recognized standards for pressure vessels, piping, hazardous materials, and electrical systems including: ASME Boiler and Pressure Vessel Code (BPVC) Section VIII for pressure-containing components; ASME B31.3 for process piping; and ISO/EN standards for microchannel and ceramic pressure systems. Where ceramics function as the primary containment, designs incorporate equivalent safety factors validated through testing.

The ammonia recovery and storage systems comply with ANSI/CGA G-2 for anhydrous ammonia, IIAR standards for refrigeration-grade ammonia handling, and NFPA 400 for hazardous materials. All ammonia handling occurs within sealed stainless-steel or alloy process lines rated for the full temperature and pressure envelope. On-site storage volumes are minimized using just-in-time synthesis and internal hydrogen use, reducing inventory-based hazards. Double-walled tanks, integrated spill containment, and gas-detection arrays provide early leak detection and automatic isolation. Ventilation and emergency scrubber systems prevent accumulation of hazardous concentrations.

The electrical systems will be specified to meet NFPA 70/NEC, IEC 60204-1, and UL 60335-2-xx standards for high-voltage industrial equipment. In the test facility controls and enclosures are rated for dust, moisture, and chemical exposure as required by IEC 60529 (IP ratings).

Azotera's design philosophy prioritizes passive safety and redundancy to minimize reliance on operator action. The systems should be passively safe in the event of a total power fault and have levels of redundancy to detect and mitigate faults while protecting equipment during operation. The system design philosophy avoids single points of failure using modular components operating in parallel with N-1 capacity. Instead of just two PSA beds alternating charging and discharging, six or 8 beds provide the improved system reliability. This allows the system to operate at capacity in the event a component module fails. The faulty membrane, or brick, compressor, or PSA bed should be replaceable without equipment downtime.

The primary operating faults posing a safety concern would include: a) an internal monolith rupture mixing fuel and oxidant streams, b) a plumbing or piping leak in the high pressure synthesis loop or c) an electrical fault or short in any of the power electronics or subsystems.

Internal monolith failures would be detected with temperature, voltage and pressure sensors, and trigger an immediate isolation of the affected drawer. Each drawer has cut-off valves, passive relief valves, and electrical disconnects along with a multitude of sensors. Different thresholds of response would halt operations in just a single drawer or begin idling the entire system. The risk mitigation includes validating the capacity of each ceramic monolith to exceed design pressure by a sufficient safety margin prior to installation.

Pressure sensors in the plumbing network would detect leaks and trigger a purge of the enclosure and idling of the operation in a single drawer, single PSA loop, single ammonia recovery loop or of the entire unit. Faults in the PSA, compressors, or refrigeration system would be quickly isolated, and ideally redundant modules would keep the system operational. If the entire PSA, refrigeration or compression systems were taken offline, the electrolysis units would enter a fast shutdown with inert purge to reach a idle operating condition that protects the electrolyzers while they cool. Back-pressure regulators and relief systems would maintain safe differential pressures between oxidant/fuel channels during the purge shutdown.